Table 1. *Postmyocardial infarction cardiomyopathy model*

	Sham (n = 4)	Vehicle (n = 4)	Ara-A (n = 12)	Ara-A + U-0126 (n = 6)
Heart rate, beats/min	386 ± 14	517 ± 12‡	520 ± 7	511 ± 13
LV ejection fraction, %	71.6 ± 1.6	42.2 ± 4.6‡	56.9 ± 1.8*	47.9 ± 1.3†
LV end diastolic diameter, mm	3.9 ± 0.2	5.6 ± 0.1‡	4.8 ± 0.1*	5.7 ± 0.2†
LV end systolic diameter, mm	2.6 ± 0.2	4.7 ± 0.2‡	3.6 ± 0.1	4.6 ± 0.1
LV wt/tibial length, mg/mm	5.1 ± 0.4	6.6 ± 0.3‡	7.1 ± 0.2	7.0 ± 0.3
Lung wt/tibial length, mg/mm	7.2 ± 0.3	12.8 ± 0.7‡	10.6 ± 0.4*	15.4 ± 0.6†

Values are means ± SE; n, no. of animals. Ara-A, adenine 9-β-D-arabinofuranoside; LV, left ventricular. $P < 0.05$, Ara-A different from vehicle (*), Ara-A + U-0126 different from Ara-A (†), and vehicle different from sham (‡).

accordance with the *Guide for the Care and Use of Laboratory Animals* (National Research Council, revised 2011). This study has been approved by the University of Medicine and Dentistry Institutional Animal Care and Use Committee.

AC assay. AC activity was measured by a modification of the method of Salomon et al. (10), as we previously described (12). When the AC assays were performed using crude membranes from AC6Tg mice heart, manganese instead of magnesium was used in the assay buffer to obtain maximum enzymatic catalytic activity because AC6 is stimulated more by manganese than by magnesium (16).

Adult cardiac myocytes. Adult cardiac myocytes were isolated from Langendorff-perfused mouse hearts as previously described (14). Enzyme solution containing 1 mg/ml collagenase (type II; Worthington), 0.1 mg/ml protease (type XIV; Sigma), and 10 μM blebbistatin (Toronto Research Chemicals) was perfused in a heart for 15–20 min followed by washing. The heart was removed from the perfusion apparatus and swirled in a culture dish. Ca^{2+} was gradually added to the dish until the concentration reached 1 mM. The cells were filtered with a cell strainer and cultured in DMEM/F-12 medium with 5% horse serum until used for the cAMP accumulation assay.

[^{3}H]adenine labeling and cAMP accumulation assay. cAMP accumulation assays in adult mouse cardiac myocytes were performed as done previously (8). Briefly, cells were incubated with [^{3}H]adenine (3 μCi/ml) for 3 h, and cells were washed and pretreated with 20 mM HEPES-balanced serum-free minimum essential medium containing 0.5 mM 3-isobutyl,1-methylxanthine. After preincubation with Ara-A for 10 min, reactions were started by the addition of 50 μM of the nonspecific AC agonist forskolin or 5 μM of the β_1/β_2-AR agonist ISO. Ten minutes after the addition of forskolin or ISO, reactions were terminated by the addition of 12% (wt/vol) trichloroacetic acid containing 0.25 mM ATP and 0.25 mM cAMP. The [^{3}H]ATP and [^{3}H]cAMP were separated with single acidic alumina columns. The cAMP production was calculated as [^{3}H]cAMP/([^{3}H]cAMP + [^{3}H]ATP) × 10^4.

ISO challenge. Mice were anesthetized with 2.5% tribromoethanol (0.015 ml/g body wt) injected intraperitoneally, and echocardiography was performed. For acute injection of ISO, a PE-10 catheter was inserted in the right jugular vein, and an ISO solution was injected at the rate of 1 μl/s. For ISO challenge experiments, Ara-A, metoprolol, or their vehicle was administered by miniosmotic pumps from 7 days before the experiment, in a dose 15 and 5 mg·kg^{-1}·day^{-1}, respectively.

Histological analyses. Heart specimens were fixed with formalin, embedded in paraffin, and sectioned at 6-μm thickness. Interstitial fibrosis was evaluated by picric acid Sirius red staining and ImagePro-Plus software analysis, as previously described (4, 10).

Western blotting. Western blotting in tissue lysate from the viable region of the left ventricle (LV) was conducted with commercially available antibodies against the phosphorylated form and total MEK or ERK (Cell Signaling). Western blotting was performed as previously described (8).

Data and statistical analysis. All data are reported as means ± SE. Statistical comparisons were calculated using a Student's t-test and ANOVA with Newman-Keuls post hoc comparison test. The groups passed the normality test and had similar variation. In addition, the Mann-Whitney test confirmed the results from the t-test for the critical data points, e.g., responses of LV ejection fraction (LVEF). Survival curves were compared using the log-rank test and Kaplan-Meier survival analysis. P values of <0.05 were considered significant.

RESULTS

AC5 inhibition decreases cAMP production in the heart. The hearts of AC5Tg mice showed a 10-fold increase in cardiac membrane AC activity using forskolin, indicating that AC5 represented most of the AC activity in the AC5Tg heart, in contrast to the wild-type (WT) or AC6Tg heart, where AC5 expression

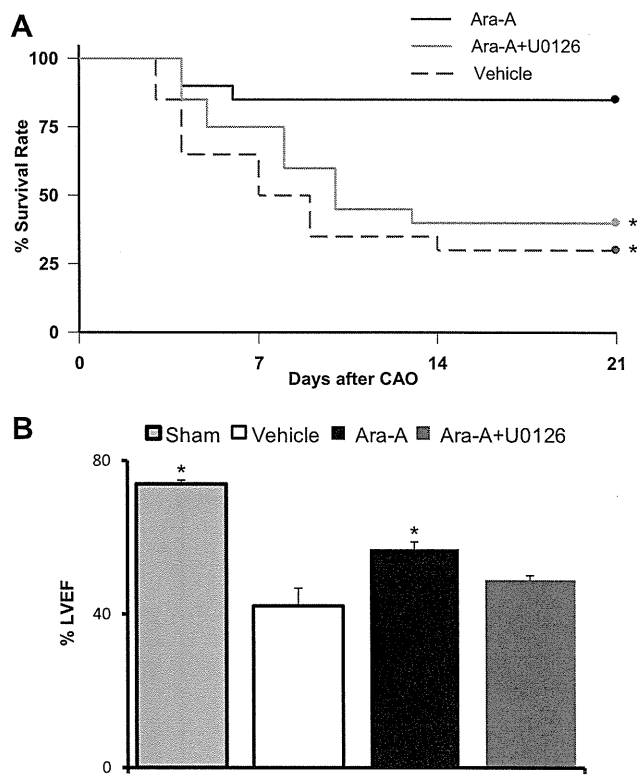

Fig. 3. Ara-A protects against postmyocardial infarction (MI) cardiomyopathy. WT C57Bl/6 mice after permanent coronary artery occlusion (CAO). *A*: follow up for 21 days. Kaplan-Meier graph of post-MI animals treated with Ara-A, Ara-A + U-0126, or vehicle. Ara-A enhanced the survival post-MI in WT C57Bl/6 mice. Log-rank test: *$P < 0.05$ vs. Ara-A, n = 16 animals/group (*B*) in survivors from experiment in *A*; LVEF was improved by Ara-A (Ara-A, n = 12; Ara-A + U-0126, n = 5; and vehicle, n = 4). U-0126 blocked the protective effects of Ara-A in terms of mortality and LVEF (*A* and *B*). t-Test: *$P < 0.05$ vs. Ara-A; †$P < 0.05$ vs. vehicle, Ara-A, or Ara-A + U-0126.

represented a relatively minor fraction of total AC. AC5KO mice showed, as expected, the null AC5 expression (9). When cardiac membrane preparations were used, Ara-A reduced cAMP production much more in AC5Tg than in WT, and not in AC5KO (Fig. 1, *A* and *B*). When cultured adult cardiac myocytes were used, Ara-A also demonstrated more effective inhibition in AC5Tg than in WT (Fig. 1, *C* and *D*). We found that the inhibitory effect was similar in WT and AC6Tg, but significantly less than observed in AC5Tg. These data suggest that Ara-A inhibits AC5, more than AC6, in the heart.

Ara-A attenuates contractile response to β-AR stimulation in AC5Tg, but little in WT. ISO was administered in mice. Ara-A did not reduce baseline LV function and reduced ISO-increased LVEF only slightly (Fig. 2*A*) in WT mice. In contrast, metoprolol depressed LV function significantly and essentially eliminated the inotropic effects of ISO challenge (Fig. 2*A*). In AC5Tg mice, the acute ISO challenge increased LVEF even more in the vehicle group, but this increased inotropic effect was not observed in the Ara-A group (Fig. 2*B*). Thus, the ability of Ara-A to block the inotropic effects of ISO is obvious only when AC5 is overexpressed. The response to ISO challenge in the AC6Tg group was similar to vehicle (Fig. 2*C*), similarly to the WT group response, further indicating the selectivity of Ara-A for AC5 (Fig. 2, *A–D*). Therefore, in contrast to metoprolol, Ara-A did not act as a β-AR blocker, i.e., did not depress cardiac function and did not eliminate the inotropic effects of ISO.

Ara-A attenuates the progression of postmyocardial infarction HF. Next, we examined the extent to which Ara-A ameliorated postmyocardial infarction (MI) cardiomyopathy. The post-MI cardiomyopathy model was induced by permanent ligation of the left anterior descending coronary artery, which results in an infarct size of 30–40% of the LV (data not shown). In this model, the LVEF was reduced significantly ($P < 0.05$, 42.2%) compared with sham (71.6%), whereas the LV end-diastolic diameter was increased ($P < 0.05$) from 3.9 in the sham to 5.6 mm in the vehicle-treated post-MI cardiomyopathy group. Lung weight/tibial length, which is an indicator of HF, was increased, $P < 0.05$, in the post-MI cardiomyopathy group (12.8) compared with the sham group (7.2) (Table 1). Ara-A improved LVEF by 38% and reduced LV diastolic end-diastolic diameter by 14% compared with the vehicle group (Fig. 3*B* and Table 1). Ara-A also significantly improved survival rate compared with vehicle ($P < 0.05$, log-rank test) (Fig. 3*A*), and reduced, $P < 0.05$, intestinal fibrosis (Fig. 4, *A* and *B*). At autopsy, the cause of death in the mice that died was either due to cardiac rupture or HF.

MEK-ERK pathway mediates the salutary effects of Ara-A. Administration of Ara-A increased the phosphorylation of MEK, ERK1, and ERK2 in WT mouse hearts (Fig. 5*A*) and in the post-MI cardiomyopathy model (Fig. 5*B*). U-0126, a MEK inhibitor, inhibited basal and Ara-A-induced ERK phosphorylation, suggesting that U-0126 indeed inhibits ERK signaling in the heart in vivo, and Ara-A activates ERK via MEK phosphorylation. U-0126 inhibited activity of MEK, but not phosphorylation itself, which is consistent with a previous report by Favata et al. (4). We found that U-0126 abolished the salutary effects of Ara-A in terms of survival (Fig. 3*A*), preservation of LV function (Fig. 3*B*), and histological evidence of fibrosis (Fig. 4, *A* and *B*).

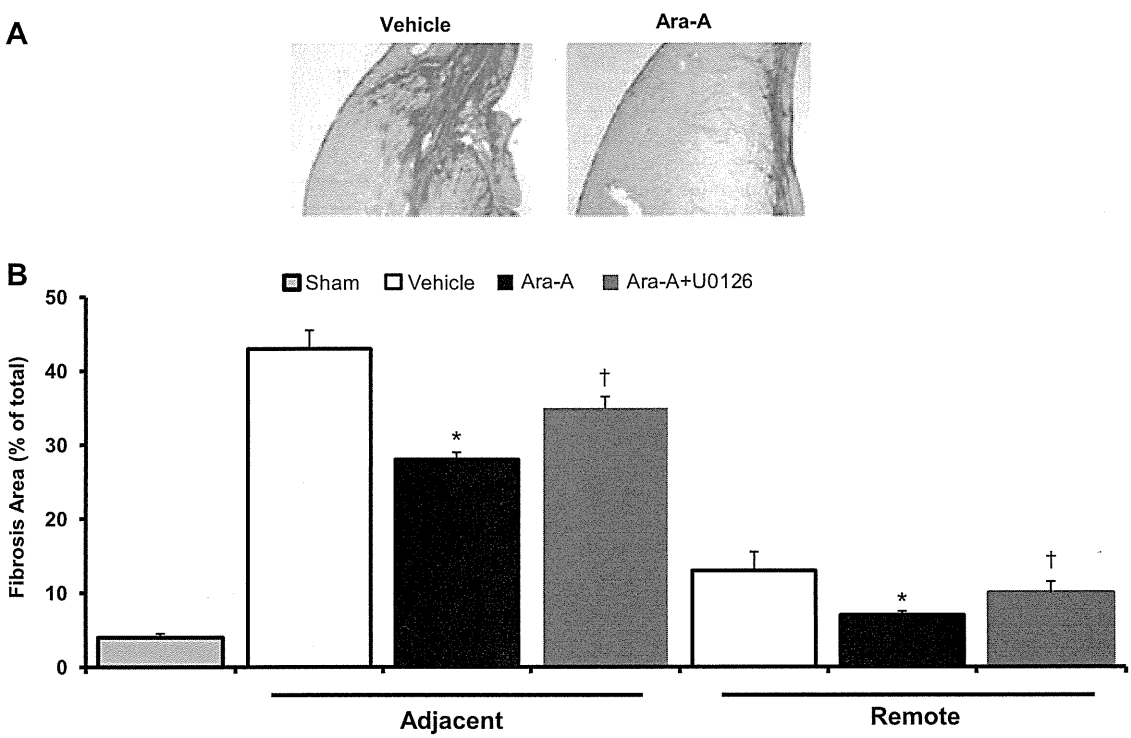

Fig. 4. Ara-A protects against cardiac fibrosis post-MI. WT C57Bl/6 mice after permanent CAO. *A*: representative images of fibrosis adjacent to infarcted myocardium with picric acid Sirius red (PASR) staining from animals treated with vehicle or Ara-A; $n = 16$ animals/group. *B*: fibrosis was increased post-MI both adjacent and remote from the infarcted area and was partially protected by Ara-A. U-0126 blocked this protection with Ara-A; vehicle group, $n = 4$; Ara-A group, $n = 10$; and Ara-A + U-0126, $n = 6$ animals. t-Test: $^*P < 0.05$ vs. vehicle; $^\dagger P < 0.05$ vs. Ara-A within the respective zone (either adjacent or remote).

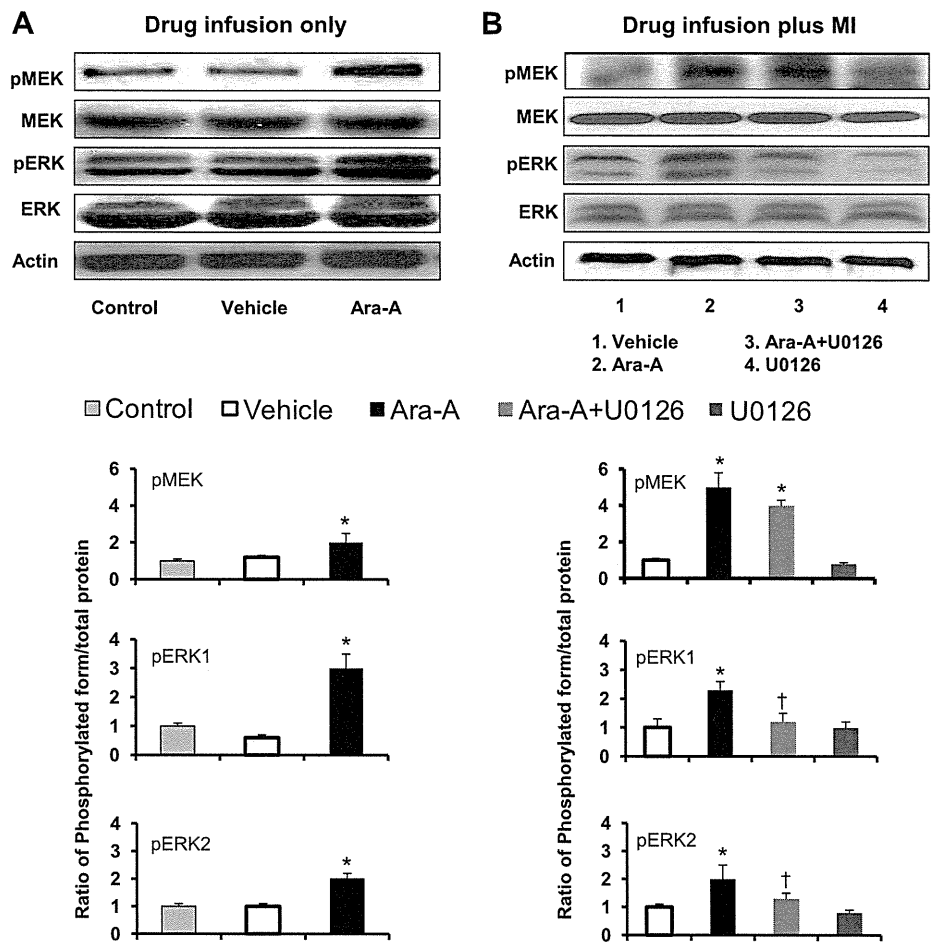

Fig. 5. Mitogen/extracellular signal-regulated kinase (MEK)/extracellular signal-regulated kinase (ERK) signaling is activated by Ara-A. *A*: Western blot analyses showed that Ara-A increased phosphorylation of MEK and ERK in the mice hearts with chronic infusion of Ara-A for 6 days. Control mice did not undergo any pump implantation. *B*: animals treated with vehicle, Ara-A, and Ara-A + U-0126 post-MI and sham were evaluated for MEK/ERK activation by Western blot. Ara-A increased ERK phosphorylation, which was inhibited by U-0126. U-0126 selectively inhibited ERK phosphorylation but not phosphorylation of MEK. The numbers at the base of *B* refer to different groups; $n = 4$ animals/group. t-Test: $^{*}P < 0.05$ vs. vehicle or vs. control; $^{\dagger}P < 0.05$ vs. Ara-A.

Ara-A preserves cardiac function with chronic catecholamine stress. We next examined whether the AC5 inhibitor, Ara-A, attenuates cardiac dysfunction induced by excessive catecholamine stress with chronic ISO infusion. Survival rate during chronic ISO infusion was higher in the Ara-A group than in the vehicle group ($P < 0.05$, log-rank test) (Fig. 6*A*). Ara-A showed preserved contractile function as measured by LVEF (Fig. 6*B*), suggesting that Ara-A protects against ISO-induced cardiac dysfunction. These data indicate that Ara-A retards the progression of ISO-induced cardiomyopathy.

DISCUSSION

There are many discoveries in genetically altered mice that cannot be applied clinically, since there is no pharmacological counterpart that can be given to animals or patients with cardiovascular disease. The major finding of this investigation is that a drug, which has been commercially available for decades, but only as an anti-viral agent, has potent and selective AC5 inhibitory properties and that this drug ameliorates the progression of cardiomyopathy in animals induced with either chronic ISO or MI. With both interventions, Ara-A demonstrated increased survival, preserved contractile dysfunction, and reduced cardiac interstitial fibrosis.

First, it was important to demonstrate that Ara-A impairs AC5 activity selectively, both in vitro and in vivo. AC5Tg showed enhanced cAMP production compared with WT, and the effects of Ara-A were greater in AC5Tg than that either in WT or in AC6Tg, which represents the other major AC isoform in the heart, indicating a high selectivity for AC5. This was supported by the data showing that Ara-A does not inhibit cAMP production in AC5KO and inhibits cAMP almost identically in AC6Tg and WT. We also examined this inhibitor in vivo and demonstrated in parallel experiments that Ara-A reduced ISO-stimulated LVEF more in AC5Tg than WT, and reduced the ISO response minimally in AC6Tg, similar to that in WT. If Ara-A was a nonselective AC inhibitor, then it should have shown enhanced AC inhibition with overexpressed AC6 as it did with overexpressed AC5. However, although we demonstrated relatively specific selectivity for AC5, and the MEK/ERK pathway, this does not mean that the inhibitor may also have other actions as well.

One could argue that Ara-A exerts its beneficial effect in ameliorating the extent of HF, simply acting as another β-AR blocker, rather than specifically on AC5, since AC5 is involved in β-AR signal transduction. We do not subscribe to this view for several reasons. First, Ara-A reduced cAMP production relatively modestly in response to ISO in WT mice in vitro and in vivo, particularly compared with the effects of metoprolol, which essentially abolished the inotropic response to ISO. Ara-A inhibited the inotropic response to ISO significantly only in the presence of elevated AC5, as in the AC5Tg, which was still less of a negative inotropic effect than metoprolol.

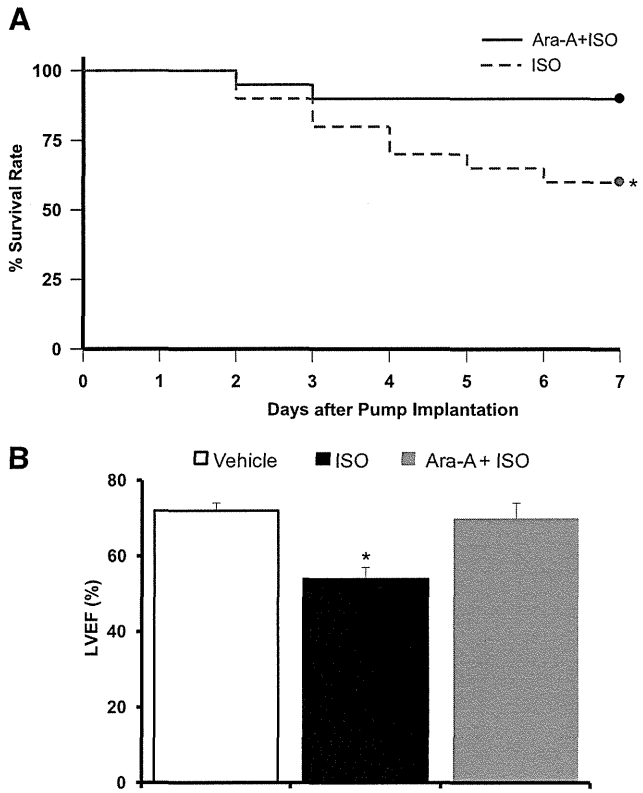

Fig. 6. AC5 inhibition attenuates chronic ISO-induced heart failure (HF). WT C57Bl/6 mice for 7 days of ISO infusion. *A*: Ara-A increased the survival rate during the period of chronic ISO infusion; $n = 32$ for ISO and $n = 18$ for the ISO + Ara-A group. *B*: Ara-A prevented LVEF dysfunction induced by chronic ISO; ISO, $n = 28$; ISO + Ara-A, $n = 16$ and vehicle, $n = 4$. t-Test: $^*P < 0.05$ vs. vehicle or vs. Ara-A + ISO.

Furthermore, the AC5 KO mouse does not show a decreased heart rate and only minimally reduced LV function (7), which is not consistent with the actions of a β-blocker. In support of this, heart rate was not lower in animals with chronic MI treated with Ara-A (Table 1).

Ara-A was previously found to inhibit AC5 activity by the computer-based drug screening system, and its inhibition was confirmed in in vitro AC assays (8). The major finding of the current investigation was to demonstrate that pretreatment with this drug ameliorated the development of HF through the MEK-ERK pathway. Thus, an anti-herpes viral drug could be used in the treatment of HF through mechanisms that have never been considered previously, i.e., inhibition of AC5. Because the animals that died after the intervention most likely suffered more severe LV dysfunction, and more animals died without treatment, then it could be argued that the salutary effects of Ara-A with both chronic ISO and post-MI may be underestimated since the mortality was also reduced.

It is important to point out that the cellular mechanism mediating the beneficial effects of Ara-A does not involve simple β-AR blockade, but rather involves MEK-ERK signaling. The link between reduced AC5 as in the AC5KO mouse and the increase in Raf-1-MEK-ERK signaling was elucidated in a prior study from our laboratory demonstrating that, in the AC5KO mouse, this pathway was involved in enhanced longevity in this mouse model (15). The current investigation demonstrates that the MEK-ERK pathway is also involved in the protection afforded in the heart by Ara-A during the development of HF and cardiac remodeling induced by MI, as evidenced by the increase in MEK-ERK signaling with Ara-A and the blockade of the salutary effects of the AC5 inhibition with the MEK inhibitor U-0126.

It is well recognized that acutely administered ISO improves LV function, whereas chronic ISO induces LV dysfunction and eventually HF along with increased mortality (1, 14). Ara-A also preserved cardiac function and reduced mortality with chronic ISO in the current study. Thus, it is tempting to speculate that pharmacological inhibition of AC5 could enhance survival in HF patients and preserve their cardiac function.

An underlying assumption of the current study is that the induction of HF, either by chronic ISO or chronic MI, induces upregulation of AC5 in the heart. Indeed this was found in a prior study in the chronic ISO model (9). This was more difficult to demonstrate in the chronic MI model in the mouse, since there is so little salvaged myocardium adjacent to the infarct. Accordingly, we examined a rat model of chronic MI and analyzed AC5 protein content, using a specific AC5 antibody (5), in myocardial samples, both adjacent and remote to the infarct. The upregulation of AC5 in the remote zone was only modest, but was more striking in the adjacent tissue (Fig. 7).

In summary, AC5 inhibition with Ara-A could be a new approach to the treatment of HF. In addition to its favorable action on halting the progression to HF due to cardiomyopathy following either permanent CAO or chronic ISO, it exerts little cardiac depression, potentially making the drug more tolerable for patients with compromised cardiac function. Importantly, since the drug studied is already FDA approved, the time from bench to bedside may be accelerated.

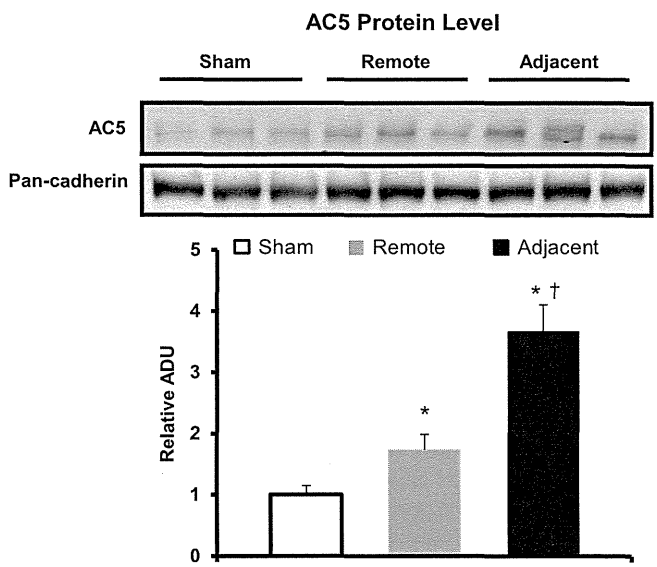

Fig. 7. AC5 protein levels are increased adjacent to infarct. Western blotting demonstrated that AC5 protein levels, assessed with a specific AC5 antibody (5), were significantly upregulated adjacent to the infarct in the chronic CAO model and less so in the remote zone. In this experiment, we used a rat model because there was not enough tissue adjacent to the infarct in the mouse chronic MI model. $^*P < 0.05$ from sham; $^\dagger P < 0.05$ from remote.

ACKNOWLEDGMENTS

This study was presented at the American Heart Association Melvin Marcus Young Investigator competition, November 2010.

GRANTS

This study is supported in part by grants from the American Heart Association (SDG 0835596D), the Foundation of the University of Medicine and Dentistry of New Jersey, the Melanoma Research Foundation, the Japanese Ministry of Health Labor and Welfare, Grant-in-Aid for Scientific Research on Innovative Areas (22136009), and National Institutes of Health Grants GM-067773, HL-102472, AG-027211, HL-033107, HL-059139, HL-069752, HL-095888, HL-069020, HL-58960, HL-062863, AG-023137, AG-014121, and AG-023567.

DISCLOSURES

No conflicts of interest are declared by the authors.

AUTHOR CONTRIBUTIONS

Author contributions: K.I., C.B., E.B., T.N., L.Y., D.E.V., S.F.V., and Y.I. conception and design of research; K.I., C.B., M. Uechi, E.B., T.N., M. Umemura, L.L., S.G., L.Y., M.P., H.Q., S.O., M.I., D.E.V., S.F.V., and Y.I. analyzed data; K.I., C.B., M. Uechi, E.B., T.N., M. Umemura, S.G., L.Y., M.P., H.Q., S.O., M.I., D.E.V., S.F.V., and Y.I. interpreted results of experiments; K.I., C.B., T.N., M. Umemura, S.G., L.Y., M.P., H.Q., M.I., D.E.V., S.F.V., and Y.I. drafted manuscript; K.I., C.B., M. Uechi, E.B., L.Y., M.P., H.Q., M.I., D.E.V., S.F.V., and Y.I. edited and revised manuscript; K.I., C.B., E.B., L.Y., D.E.V., S.F.V., and Y.I. approved final version of manuscript; C.B., M. Uechi, E.B., T.N., M. Umemura, L.L., S.G., X.Z., M.P., H.Q., S.O., and M.I. performed experiments; C.B., M. Uechi, E.B., T.N., M. Umemura, L.L., S.G., L.Y., M.P., H.Q., S.O., and M.I. prepared figures.

REFERENCES

1. **Balakumar P, Singh AP, Singh M.** Rodent models of heart failure. *J Pharmacol Toxicol Methods* 56: 1–10, 2007.
2. **Bristow MR.** beta-adrenergic receptor blockade in chronic heart failure. *Circulation* 101: 558–569, 2000.
3. **Depre C, Wang L, Sui X, Qiu H, Hong C, Hedhli N, Ginion A, Shah A, Pelat M, Bertrand L, Wagner T, Gaussin V, Vatner SF.** H11 kinase prevents myocardial infarction by preemptive preconditioning of the heart. *Circ Res* 98: 280–288, 2006.
4. **Favata MF, Horiuchi KY, Manos EJ, Daulerio AJ, Stradley DA, Feeser WS, Van Dyk DE, Pitts WJ, Earl RA, Hobbs F, Copeland RA, Magolda RL, Scherle PA, Trzaskos JM.** Identification of a novel inhibitor of mitogen-activated protein kinase kinase. *J Biol Chem* 273: 18623–18632, 1998.
5. **Hu CL, Chandra R, Ge H, Pain J, Yan L, Babu G, Depre C, Iwatsubo K, Ishikawa Y, Sadoshima J, Vatner SF, Vatner DE.** Adenylyl cyclase type 5 protein expression during cardiac development and stress. *Am J Physiol Heart Circ Physiol* 297: H1776–H1782, 2009.
6. **Iwatsubo K, Minamisawa S, Tsunematsu T, Nakagome M, Toya Y, Tomlinson JE, Umemura S, Scarborough RM, Levy DE, Ishikawa Y.** Direct inhibition of type 5 adenylyl cyclase prevents myocardial apoptosis without functional deterioration. *J Biol Chem* 279: 40938–40945, 2004.
7. **Okumura S, Kawabe J, Yatani A, Takagi G, Lee MC, Hong C, Liu J, Takagi I, Sadoshima J, Vatner DE, Vatner SF, Ishikawa Y.** Type 5 adenylyl cyclase disruption alters not only sympathetic but also parasympathetic and calcium-mediated cardiac regulation. *Circ Res* 93: 364–371, 2003.
8. **Okumura S, Takagi G, Kawabe J, Yang G, Lee MC, Hong C, Liu J, Vatner DE, Sadoshima J, Vatner SF, Ishikawa Y.** Disruption of type 5 adenylyl cyclase gene preserves cardiac function against pressure overload. *Proc Natl Acad Sci USA* 100: 9986–9990, 2003.
9. **Okumura S, Vatner DE, Kurotani R, Bai Y, Gao S, Yuan Z, Iwatsubo K, Ulucan C, Kawabe J, Ghosh K, Vatner SF, Ishikawa Y.** Disruption of type 5 adenylyl cyclase enhances desensitization of cyclic adenosine monophosphate signal and increases Akt signal with chronic catecholamine stress. *Circulation* 116: 1776–1783, 2007.
10. **Salomon Y, Londos C, Rodbell M.** A highly sensitive adenylate cyclase assay. *Anal Biochem* 58: 541–548, 1974.
11. **Szabó J, Csáky L, Szegi J.** Experimental cardiac hypertrophy induced by isoproterenol in the rat. *Acta Physiol Acad Sci Hung* 46: 281–285, 1975.
12. **Tamaoki J, Tagaya E, Kawatani K, Nakata J, Endo Y, Nagai A.** Airway mucosal thickening and bronchial hyperresponsiveness induced by inhaled beta 2-agonist in mice. *Chest* 126: 205–212, 2004.
13. **Whitley RJ, Alford CA, Hirsch MS, Schooley RT, Luby JP, Aoki FY, Hanley D, Nahmias AJ, Soong SJ.** Vidarabine versus acyclovir therapy in herpes simplex encephalitis. *N Engl J Med* 314: 144–149, 1986.
14. **Xie LH, Chen F, Karagueuzian HS, Weiss JN.** Oxidative-stress-induced afterdepolarizations and calmodulin kinase II signaling. *Circ Res* 104: 79–86, 2009.
15. **Yan L, Vatner DE, O'Connor JP, Ivessa A, Ge H, Chen W, Hirotani S, Ishikawa Y, Sadoshima J, Vatner SF.** Type 5 adenylyl cyclase disruption increases longevity and protects against stress. *Cell* 130: 247–258, 2007.
16. **Yoo B, Iyengar R, Chen Y.** Functional analysis of the interface regions involved in interactions between the central cytoplasmic loop and the C-terminal tail of adenylyl cyclase. *J Biol Chem* 279: 13925–13933, 2004.

Circulation Journal
Official Journal of the Japanese Circulation Society
http://www.j-circ.or.jp

ORIGINAL ARTICLE
Pediatric Cardiology and Adult Congenital Heart Disease

Inhibition of Phosphodiesterase Type 3 Dilates the Rat Ductus Arteriosus Without Inducing Intimal Thickening

Yasuhiro Ichikawa, MD; Utako Yokoyama, MD, PhD; Mari Iwamoto, MD, PhD; Jin Oshikawa, MD, PhD; Satoshi Okumura, MD, PhD; Motohiko Sato, MD, PhD; Shumpei Yokota, MD, PhD; Munetaka Masuda, MD, PhD; Toshihide Asou, MD, PhD; Yoshihiro Ishikawa, MD, PhD

Background: Prostaglandin E_1 (PGE_1), via cAMP, dilates the ductus arteriosus (DA). For patients with DA-dependent congenital heart disease (CHD), PGE_1 is the sole DA dilator that is used until surgery, but PGE_1 has a short duration of action, and frequently induces apnea. Most importantly, PGE_1 increases hyaluronan (HA) production, leading to intimal thickening (IT) and eventually DA stenosis after long-term use. The purpose of this study was therefore to investigate potential DA dilators, such as phosphodiesterase 3 (PDE3) inhibitors, as alternatives to PGE_1.

Methods and Results: Expression of PDE3a and PDE3b mRNAs in rat DA tissue was higher than in the pulmonary artery. I.p. milrinone (10 or 1 mg/kg) or olprinone (5 or 0.5 mg/kg) induced maximal dilatation of the DA lasting for up to 2 h in rat neonates. In contrast, vasodilation induced by PGE_1 (10 μg/kg) was diminished within 2 h. No respiratory distress was observed with milrinone or olprinone. Most important, milrinone did not induce HA production, cell migration, or proliferation when applied to cultured rat DA smooth muscle cells. Further, high expression of both PDE3a and PDE3b was demonstrated in the human DA tissue of CHD patients.

Conclusions: Because PDE3 inhibitors induced longer-lasting vasodilation without causing apnea or HA-mediated IT, they may be good alternatives to PGE_1 for patients with DA-dependent CHD. (*Circ J* 2012; **76:** 2456–2464)

Key Words: Congenital heart disease; Ductus arteriosus; Milrinone; Phosphodiesterase

The ductus arteriosus (DA), the fetal arterial connection between the pulmonary artery (PA) and the descending aorta, is essential to maintain fetal life in utero. The DA closes after birth by 2 different mechanisms: vasoconstriction and intimal thickening (IT).[1–3] During the first few hours after birth, acute vasoconstriction occurs as a result of smooth muscle contraction in the DA. This is triggered by increased oxygen tension, due to the initiation of spontaneous breathing, and decreased circulating prostaglandin E_2 (PGE_2), due to disconnection from the placenta.[3] This functional vasoconstriction, however, must be preceded by IT of the DA, because vascular remodeling, including IT, is critical for anatomical closure of the DA.

The IT of the DA is a result of many cellular processes, such as an increase in smooth muscle cell (SMC) migration and proliferation, the production of hyaluronan (HA) under the endothelial layer, and decreased elastin fiber assembly.[1,3,4] We have previously demonstrated that PGEs promoted HA production via cAMP/protein kinase A and subsequent SMC migration, resulting in IT of the DA during the late gestational period.[1,4,5] In patients with DA-dependent congenital heart disease (CHD), such as pulmonary atresia with intact ventricular septum or arch anomalies (coarctation of aorta or interruption of aortic arch), however, patent DA after birth is essential for survival.

PGE_1 is widely used to keep the DA open because it increases intracellular cAMP and thus dilates the DA. But PGE_1 induces HA-mediated IT and thus DA stenosis after prolonged use.[6] The fact that it induces only a very short duration of vasodilation, together with its severe adverse effects, such as apnea, respiratory distress, and hypotension, present additional problems, making it difficult for some patients with CHD to

Received February 16, 2012; revised manuscript received May 10, 2012; accepted June 4, 2012; released online July 6, 2012 Time for primary review: 13 days

Cardiovascular Research Institute (Y. Ichikawa, U.Y., S.O., M.S., Y. Ishikawa), Department of Pediatrics (Y. Ichikawa, M.I., S.Y.), Medical Science and Cardiorenal Medicine (J.O.), Department of Surgery (M.M.), Yokohama City University, Yokohama; and Department of Cardiovascular Surgery, Kanagawa Children's Medical Center, Yokohama (T.A.), Japan

Mailing address: Utako Yokoyama, MD, PhD or Yoshihiro Ishikawa, MD, PhD, Cardiovascular Research Institute, Yokohama City University, 3-9 Fukuura, Kanazawa-ku, Yokohama 236-0004, Japan. E-mail: utako@yokohama-cu.ac.jp or yishikaw@med.yokohama-cu.ac.jp

ISSN-1346-9843 doi:10.1253/circj.CJ-12-0215

continue the use of PGE_1 until surgery. As such, possible alternatives to PGE_1 need to be investigated.

Phosphodiesterases (PDEs), which catalyze the hydrolysis of cAMP/cGMP, constitute a superfamily of at least 11 gene families (PDE1–PDE11).[7] The 2 PDE3 subfamilies, PDE3A and PDE3B, are encoded by closely related genes,[8] and both hydrolyze cAMP. PDE3 inhibitors have been approved by the US Food and Drug Administration (FDA) for use as vasodilators as well as in heart failure. Two of these are milrinone and olprinone, which are widely used to treat heart failure[9–12] and persistent pulmonary hypertension in neonates.[13,14] Previous studies have shown that the PDE3 inhibitors milrinone, amrinone, and cilostazol counteract indomethacin-induced DA contraction.[15,16] Thus, PDE3 inhibitors alone may be sufficient to dilate the DA. Nevertheless, it remains undetermined whether they induce IT, which is a major problem with PGE_1, via HA production, cell migration, or cell proliferation. In the current study, we investigated the role of PDE3 inhibitors in DA vascular remodeling and vasodilation with a view to their potential use as alternatives to the current PGE therapy.

Methods

Animals and Materials

Timed pregnant Wistar rats were purchased from Japan SLC (Hamamatsu, Japan). All animal studies were approved by the institutional animal care and use committees of Yokohama City University. Milrinone, platelet derived growth factor-BB (PDGF-BB), 3-[4,5-dimethylthiazol-2-yl]-2,5-diphenyltetrazolium bromide (MTT), trichloroacetic acid, and 10% buffered formalin were obtained from Wako (Osaka, Japan). Olprinone, cilostazol, rolipram, PGE_1, PGE_2, elastase type II, trypsin inhibitor, bovine serum albumin V, poly-L-lysine, penicillin-streptomycin solution, acetic anhydride, triethylamine, Dulbecco's modified Eagle's medium (DMEM), and Hank's balanced salt solution (HBSS) were purchased from Sigma-Aldrich (St Louis, MO, USA). Collagenase II was purchased from Worthington Biochemical (Lakewood, NJ, USA). Collagenase/dispase was purchased from Roche Diagnostics (Tokyo, Japan). Fetal bovine serum (FBS) was purchased from Equitech-Bio (Kerrville, TX, USA).

Primary Culture of Rat SMCs

Vascular SMCs in primary culture were obtained from the DA (DASMCs), the aorta (ASMCs), and the PAs (PASMCs) of Wistar rats on the 21st day of gestation. Isolation of DASMCs and ASMCs has been described previously.[17] To obtain PASMCs, the branch extralobular PAs were dissected, cleaned from adherent tissue, and cut into small pieces. The tissues were transferred to a 1.5-ml centrifuge tube that contained 800 μl of collagenase-dispase enzyme mixture (1.5 mg/ml collagenase-dispase, 0.5 mg/ml of elastase type II-A, 1 mg/ml of trypsin inhibitor type I-S, and 2 mg/ml of bovine serum albumin fraction V in HBSS). Digestion was carried out at 37°C for 15 min. Cell suspensions were then centrifuged, and the medium was changed to a collagenase II enzyme mixture (1 mg/ml collagenase II, 0.3 mg/ml trypsin inhibitor type I-S, and 2 mg/ml bovine serum albumin fraction V in HBSS). After 12 min of incubation at 37°C, cell suspensions were transferred to growth medium in 35-mm poly-L-lysine-coated dishes in a moist tissue culture incubator at 37°C in 5% CO_2-95% ambient mixed air. The growth medium contained DMEM with 10% FBS, 100 U/ml penicillin, and 100 mg/ml streptomycin. We confirmed that >99% of cells were positive for α-smooth muscle actin and exhibited typical hill-and-valley morphology. Expression of PDE3, prostaglandin E receptor EP4 (EP4), and prostacyclin (IP) receptor mRNAs in DASMCs, ASMCs, and PASMCs is shown in Figure S1.

Table. Patient Characteristics

Patient no.	Age at operation	Diagnosis
1	0 days	Asplenia, PA, TAPVD, CA, SV
2	1 day	Asplenia, CoA, CA, SV
3	2 days	IAA, Aorticopulmonary window
4	2 days	CoA, VSD
5	3 days	TGA, CoA
6	4 days	CoA, VSD
7	13 days	CoA, VSD
8	1 month	HypoLV, CoA, VSD

CA, common atrium; CoA, coarctation of the aorta; hypoLV, hypoplastic left ventricle; IAA, interruption of aortic arch; PA, pulmonary atresia; SV, single ventricle; TAPVD, total anomalous pulmonary venous drainage; TGA, transposition of the great arteries; VSD, ventricular septal defect.

Human Tissue From CHD Patients

We obtained 8 neonatal DAs and adjacent aortas during cardiac surgery in children between 0 days and 1 month of age. All excised tissue was fixed in 4% paraformaldehyde within 3 h. The DA tissues were obtained from the Yokohama City University Hospital and Kanagawa Children's Medical Center. The study was approved by the human subject committees at both Yokohama City University and Kanagawa Children's Medical Center. Detailed patient information is summarized in Table.

RNA Isolation and Quantitative Reverse Transcription-Polymerase Chain Reaction (RT-PCR)

Pooled vascular tissues were obtained from Wistar rats on the 21st day of gestation. After excision, tissues were frozen in liquid nitrogen and stored at –80°C. The total RNA was isolated from the tissues using an RNeasy Mini Kit (Qiagen, Valencia, CA, USA) according to the manufacturer's instructions and from the cultures using Trizol reagent (Invitrogen, Carlsbad, CA, USA). The primers were designed based on the rat nucleotide sequences of PDE3a (NM_017337) (5'-CGC CTG AGA AGA AGT TTG C-3' and 5'-AGA CAG CAT AGG ACG AAG TGA AG-3'), PDE3b (NM_017229.1) (5'-TCC AAA GCA GAG GTC ATC ATC-3' and 5'-GTA TCA AGA AAT CCT ACG GGT GA-3'), EP4 (NR_032076.3) (5'-CTC GTG GTG CGA GTG TTC AT-3' and 5'-AAG CAA TTC TGA TGG CCT GC-3'), and IP (NM_00177644.1) (5'-GGG CAC GAG AGG ATG AAG-3' and 5'-GGG CAC ACA GAC AAC ACA AC-3'). RT-PCR was performed using a PrimeScript RT reagent Kit (TaKaRa Bio, Tokyo, Japan) and real-time PCR was performed using SYBR Green (Applied Biosystems, Foster City, CA, USA). The abundance of each gene was determined relative to that in 18S ribosomal RNA.

Rapid Whole-Body Freezing Method

To study the in situ morphology and inner diameter of the neonatal DA, a rapid whole-body freezing method was used as previously described.[2] Fetuses on the 21st day of gestation were delivered by cesarean section, and immediately after birth i.p. injections of milrinone (10 mg/kg, 1 mg/kg, 0.1 mg/kg), olprinone (5 mg/kg, 0.5 mg/kg, 0.05 mg/kg), or PGE_1 (10 μg/kg) were given. The rat pups were frozen in liquid nitrogen at 0,

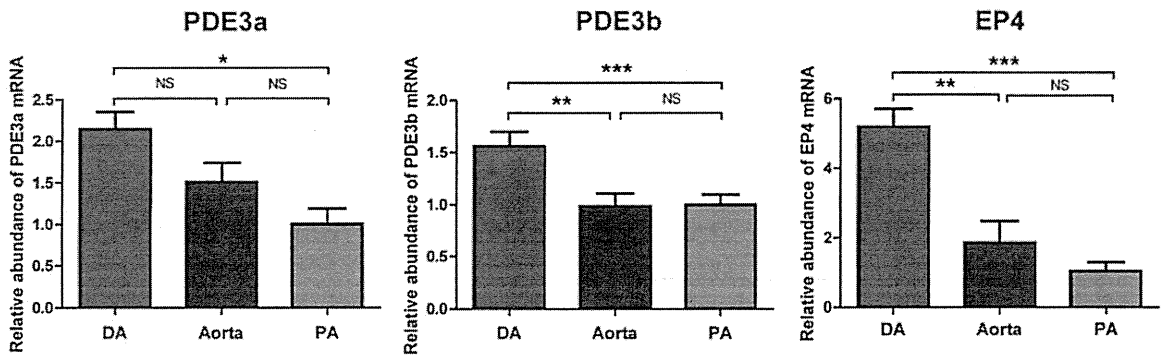

Figure 1. Quantitative reverse transcription-polymerase chain reaction (RT-PCR) of PDE3a, PDE3b, and EP4 in rat ductus arteriosus (DA), aorta, and pulmonary artery (PA) tissue on the 21st day of gestation. n=4–5. *P<0.05; **P<0.01; ***P<0.001. PDE, phosphodiesterase; NS, not significant.

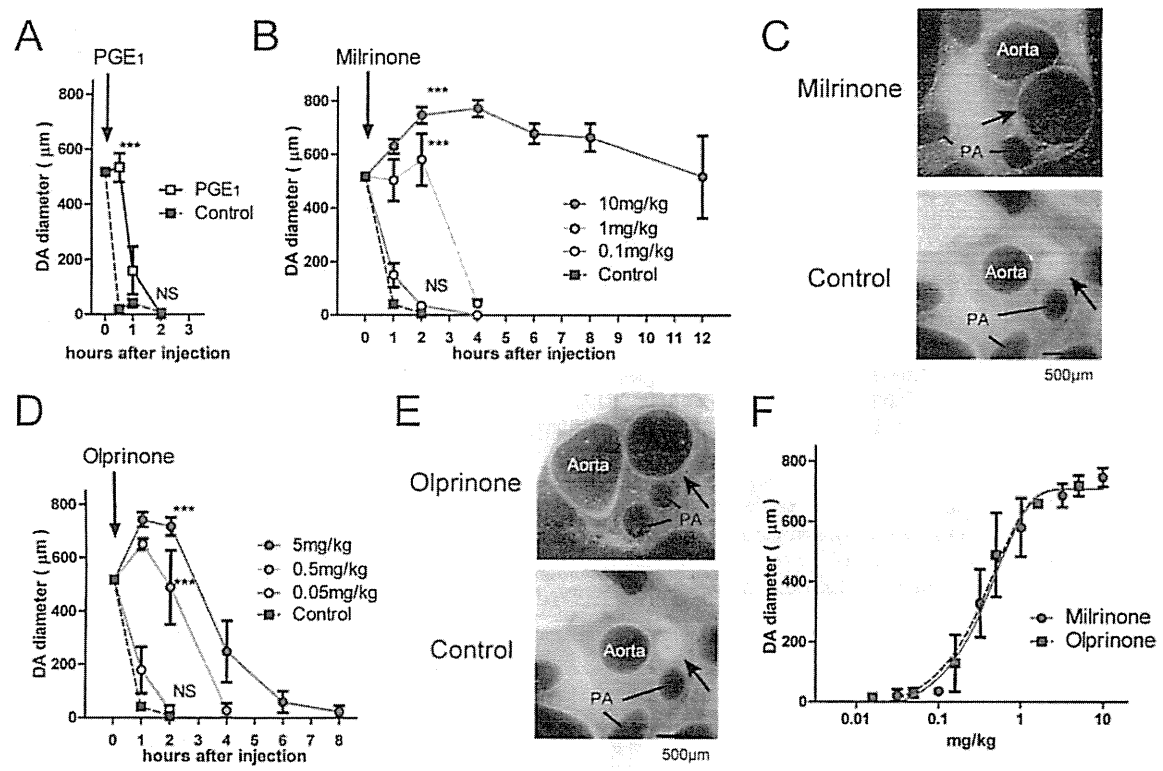

Figure 2. Effects of milrinone and olprinone on vasodilation of the ductus arteriosus (DA) as observed using the rapid whole-body freezing method. (A) Prostaglandin E_1 (PGE_1; 10μg/kg)-induced dilation of rat DA (n=4–6). (B) Vasodilatory effect of milrinone on rat DA. Rat neonates were injected i.p. with milrinone (n=4–6). (C) Representative images of rat DAs treated with 10mg/kg of milrinone or saline (control) for 2h using the whole-body freezing method (arrow). (D) Vasodilatory effect of milrinone on rat DA. Rat neonates were injected i.p. with olprinone (n=4–6). (E) Representative images of rat DAs treated with 5mg/kg of olprinone or control for 2h using the whole-body freezing method (arrow). (F) Milrinone or olprinone dilated DA in a dose-dependent manner. Vasodilatory effects of phosphodiesterase 3 (PDE3) inhibitors were examined 2h after injection (n=4–6). ***P<0.001 and NS vs. control. NS, not significant.

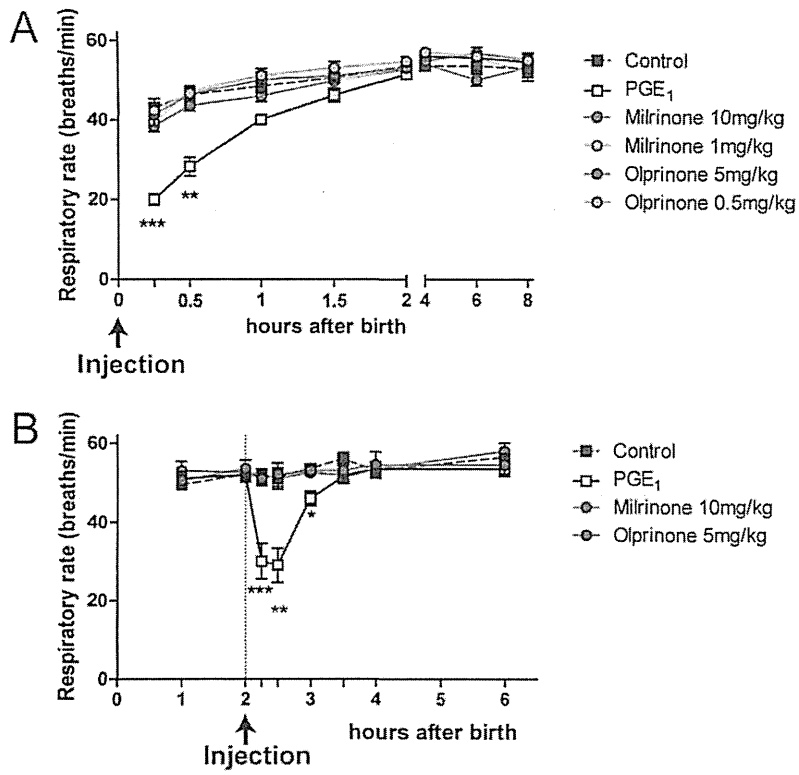

Figure 3. Effects of phosphodiesterase 3 (PDE3) inhibitors and prostaglandin E_1 (PGE_1) on respiratory distress. (A) Respiratory rate of rat neonates given each drug immediately after birth, the same as in Figure 2 (n=6–9). (B) Respiratory rate of rat neonates given each drug 2h after birth (n=4). *P<0.05, **P<0.01 and ***P<0.001 vs. control. No mark, not significant vs. control.

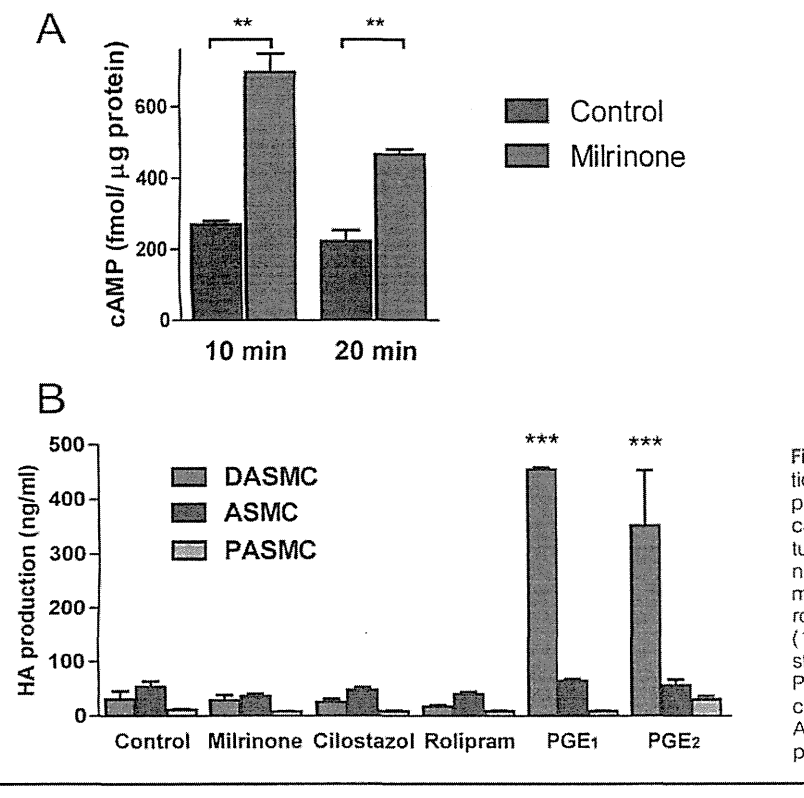

Figure 4. Milrinone increased cAMP production, but it did not induce hyaluronan (HA) production. (A) Milrinone (10 μmol/L) significantly increased cAMP accumulation in ductus arteriosus smooth muscle cells (DASMCs; n=4). (B) HA production in SMCs treated with milrinone (10 μmol/L), cilostazol (10 μmol/L), rolipram (10 μmol/L), prostaglandin (PG)E_1 (1 μmol/L), or PGE_2 (1 μmol/L; n=4–6). Cilostazol, phosphodiesterase 3 (PDE3); Rolipram, PDE4 inhibitor. **P<0.01 and ***P<0.001 vs. control. No mark, not significant vs. control. ASMCs, aortic smooth muscle cells; PASMCs, pulmonary artery smooth muscle cells.

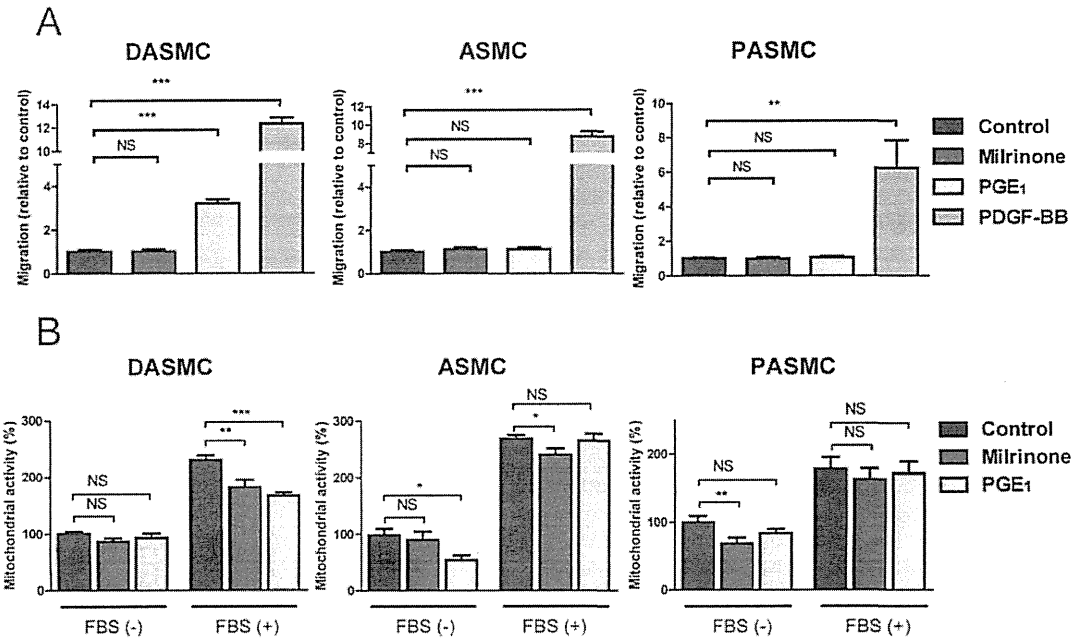

Figure 5. Milrinone did not promote migration and proliferation in smooth muscle cells (SMCs). (A) Migration of SMCs treated with milrinone (10 μmol/L), prostaglandin E1 (PGE1; 1 μmol/L), or platelet derived growth factor-BB (PDGF-BB; 10 ng/ml) using the Boyden chamber method (n=4–5). (B) Proliferation of SMCs treated with milrinone (10 μmol/L) or PGE1 (1 μmol/L) in the presence of 0 or 10% fetal bovine serum (FBS) on MTT assay (n=5–9). *P<0.05, **P<0.01 and ***P<0.001. NS, not significant. ASMCs, aortic smooth muscle cells; DASMCs, ductus arteriosus smooth muscle cells; PASMCs, pulmonary artery smooth muscle cells.

0.5, 1, 2, 4, 6, 8, and 12 h after injection. The frozen thoraxes were then cut on a microtome, and the inner diameter of each DA was measured.

Determination of Respiratory Rate

Fetuses on the 21st day of gestation were delivered by cesarean section, and at 0 or 2 h after birth i.p. injections of milrinone (10 mg/kg, 1 mg/kg), olprinone (5 mg/kg, 0.5 mg/kg), or PGE1 (10 μg/kg) were given. We measured the respiratory rate by counting the movements of the rat thorax.

Quantification of HA

The amount of HA in the cell culture supernatant was measured according to the latex agglutination method as previously described.[1]

SMC Migration Assay

The migration assay was performed using 24-well transwell culture inserts with polycarbonate membranes (8-μm pores; Corning, Corning, NY, USA) as previously described.[1] Cells were stimulated with milrinone (10 μmol/L), PGE1 (1 μmol/L), PDEF-BB (10 ng/ml), HA (200 ng/ml), or milrinone+HA for 3 days.

Cell Proliferation Assay

SMCs were cultured on 24-well plates at 1×10^5 cells per well in DMEM supplemented with 10% FBS. After various treatments over 3 days, 500 μl of 1 mg/ml MTT solution was added to each well and incubated for 2 h. The supernatants were aspirated, and the formazan crystals in each well were solubilized with 0.05 mol/L HCl (500 μl). Each solution (100 μl) was placed in a 96-well plate. SMC proliferation was measured based on absorbance at 570 nm using a microplate reader.

Immunohistochemistry

Immunohistochemical analysis was performed as previously described.[1,18] Rabbit polyclonal anti-PDE3A antibody (sc-20792) and goat polyclonal anti-PDE3b antibody (sc-11835) were purchased from Santa Cruz Biotechnology (Santa Cruz, CA, USA). A color extraction method using BIOREVO bz-9000 (KEYENCE, Osaka, Japan) was performed to quantify the expression of PDE3 s in the DAs and the aortas of patients 1, 4, 5, and 8 (Table). Eighteen fields in the smooth muscle layer of the DA and the aorta respectively were examined in 4 cases. On diaminobenzidine staining, PDE3a-positive or PDE3b-positive areas were extracted and counted on the screen.

Radioimmunoassay Measurement of Cyclic AMP Production

Measurement of cAMP accumulation in DASMCs was performed as previously described.[2,19] Briefly, DASMCs grown on 24-well plates were serum-starved for 24 h and assayed for cAMP production after a 10- or 20-min period of incubation with 10 μmol/L of milrinone. Reactions were terminated by aspiration of the media and the addition of 300 μl of ice-cold trichloroacetic acid (7.5%) to each well. Forty microliters of each sample were acetylated and incubated with ^{125}I-cAMP (Perkin Elmer, Waltham, MA, USA) and 50 μl of rabbit anti-cAMP antibody (diluted 1:3,000, Millipore, Billerica, MA, USA) overnight at 4°C. Each mixture was then incubated with

50 μl of goat anti-rabbit antibody with magnetic beads (Qiagen) for 1 h. Separation of bound antibodies from free antibodies was achieved by filtration, and bound radioactivity was counted. Production of cAMP was normalized to the amount of protein per sample.

Statistical Analysis

Data are presented as mean±SEM of independent experiments. Statistical analysis was performed between 2 groups using unpaired 2-tailed Student's t-test or unpaired t-test with Welch's correction, and among multiple groups using 1-way analysis of variance followed by Tukey's multiple comparison test. $P<0.05$ was considered significant.

Results

Messenger RNA of PDE3 Isoforms Highly Expressed in Rat DA

We first examined whether the target molecule of PDE3 inhibitors is highly expressed in the DA. We measured the mRNA expression of PDE3s using quantitative RT-PCR in the rat DA, aorta, and PA on the 21st day of gestation (Figure 1). Expression of PDE3a mRNA was higher in the DA than in the PA. Expression of PDE3b mRNA was higher in the DA than in the aorta or the PA. We also confirmed that EP4 mRNA was more highly expressed in the DA than in the aorta or the PA. Thus, PDE3 isoforms were abundantly expressed in the DA relative to the PA.

Vasodilatory Effects of PDE3 Inhibitors on Rat DA In Vivo

PDE3 inhibitors are widely used in neonates and children with low cardiac output following myocarditis and cardiovascular surgery for CHD.[20,21] We examined whether milrinone or olprinone dilated the DA using the rapid whole-body freezing method in rat neonates. Neonates were injected with 1 of these drugs immediately after birth to mimic the vasodilatory treatment currently used in DA-dependent CHD.

I.p. injection of PGE_1 (10 μg/kg, the amount that is given i.v. daily as a clinical maintenance dose) induced maximum dilatation of the DA for 30 min, but this effect was completely lost within 2 h after injection (Figure 2A). A single i.p. injection of 10 mg/kg of milrinone maintained maximum dilation of the DA for up to 12 h (Figures 2B,C); 1 mg/kg of milrinone, the amount that is given i.v. daily as a clinical maintenance dose, maintained maximum dilatation for 2 h, after which DA closure occurred at 4 h after injection. And 0.1 mg/kg of milrinone did not affect DA tone. Both 5 mg/kg and 0.5 mg/kg of olprinone, the latter of which is suitable for daily i.v. use as a clinical maintenance dose, induced maximum dilatation for 1 h after injection (Figures 2D,E). A dose of 0.05 mg/kg olprinone did not dilate the DA. Thus, both milrinone and olprinone produced dose-dependent vasodilatory effects (Figure 2F), but those of milrinone lasted longer.

PDE3 Inhibitors Do Not Induce Respiratory Distress

Given that respiratory distress is a major adverse effect of PGE_1,[22] we examined whether PDE3 inhibitors cause respiratory distress. We measured the respiratory rate of rat neonates given milrinone, olprinone, or PGE_1. When rat neonates were given each drug immediately after birth, PGE_1 significantly reduced the respiratory rate at 15 or 30 min after injection, *whereas* milrinone (1 and 10 mg/kg) and olprinone (0.5 and 5 mg/kg) did not induce respiratory distress up to 8 h after injection compared to the saline control (Figure 3A). To exclude the possibility that neonates given PGE_1 had a congenital respiratory problem, we examined the effect of drugs using a different injection timing. We confirmed that all rat neonates had established normal breathing 1 h after birth, and then each drug was given. PGE_1 significantly reduced the respiratory rate up to 1 h after injection. In contrast, milrinone (10 mg/kg) and olprinone (5 mg/kg) did not affect the respiratory rate compared to the control (Figure 3B). These data suggest that PDE3 inhibitors did not cause respiratory distress.

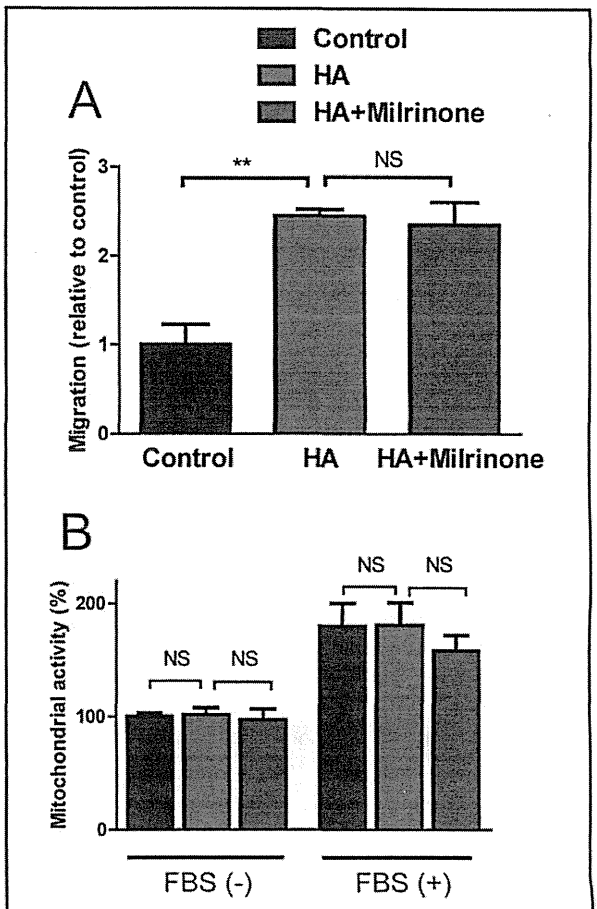

Figure 6. Effect of co-treatment of hyaluronan (HA) with milrinone on migration and proliferation in ductus arteriosus smooth muscle cells (DASMCs). (A) Migration of SMCs with co-treatment of HA (200 ng/ml) and milrinone (10 μmol/L) using the Boyden chamber method (n=4–5). (B) Proliferation of SMCs with co-treatment of HA (200 ng/ml) and milrinone (10 μmol/L) in the presence of 0 or 10% fetal bovine serum (FBS) on MTT assay (n=8). **P<0.01. NS, not significant.

Milrinone Do Not Promote HA Production or SMC Migration and Proliferation

Although it was previously suggested that PDE3 inhibitors induced vasodilation of the DA, it remained unknown whether they also induced IT formation, a key process in the anatomical closure of the DA. It is known that PGEs stimulate HA production along with increased DASMC migration through the action of HA as a potent trigger of cell migration. This is the major mechanism underlying the increase in IT induced by PGEs.[1,2,5]

We thus examined whether a PDE3 inhibitor, milrinone,

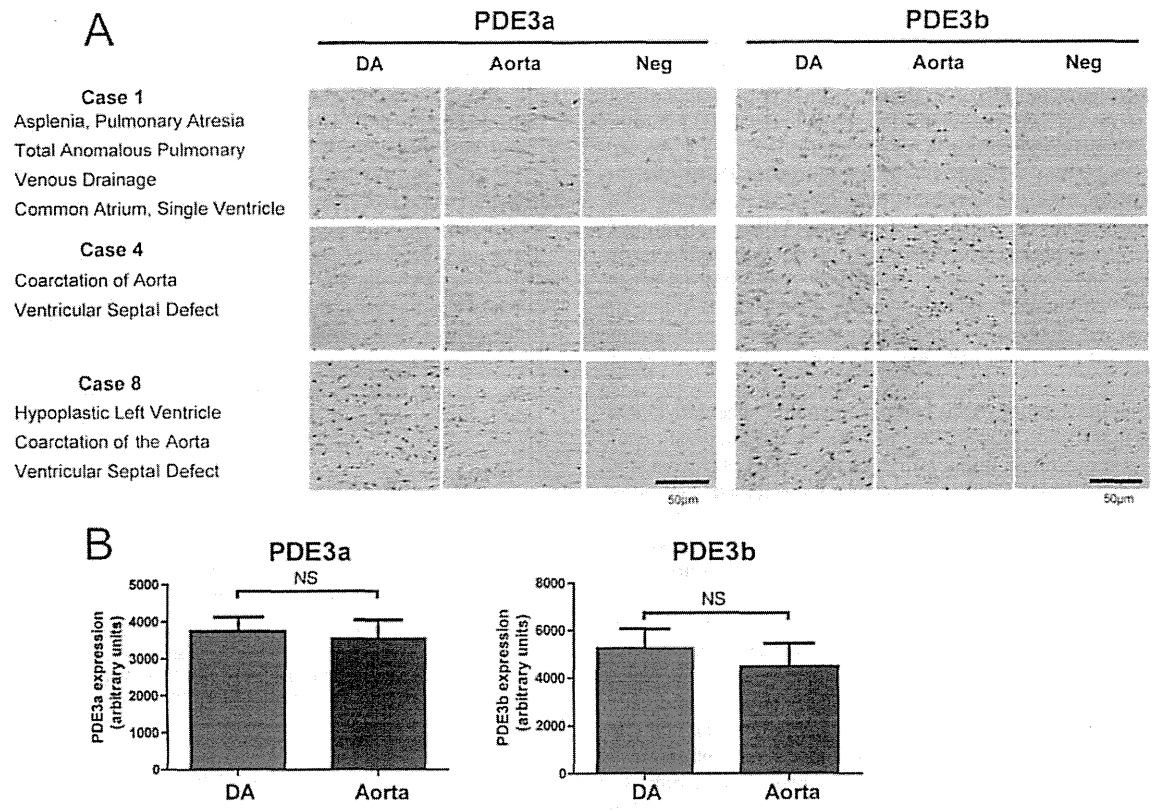

Figure 7. (A) Representative images of immunoreaction to PDE3a and PDE3b in the human ductus arteriosus (DA) and aortic smooth muscle layers according to type of congenital heart disease. No immunoreaction was detected when omitting the primary antibody, as in PDE3a Neg and PDE3b Neg. (B) Quantification of PDE3a and PDE3b in the DA and the aorta using a color extraction method (n=4). PDE, phosphodiesterase; NS, not significant.

regulated HA production or SMC migration. First, we confirmed cAMP production in the presence of milrinone. Milrinone significantly increased cAMP accumulation in DASMCs at a dosage of 10 μmol/L, which also induced marked dilatation of DA explants (Figure 4A).[16] But the same dosage of milrinone (10 μmol/L) did not induce HA production in DASMCs (Figure 4B). We also confirmed that the PDE3 inhibitor cilostazol did not induce HA production in DASMCs. Similarly, PGE_1 (1 μmol/L) induced DASMC migration; but milrinone did not increase DASMC migration, as determined using the Boyden chamber method (Figure 5A). The cells used for these tests were sufficiently stimulated with PGE_1 to induce HA production and with PDGF-BB to induce migration. Next, we examined the effects of a PDE3 inhibitor on SMC proliferation, because SMC proliferation plays a role in IT formation of the DA.[23,24] Milrinone and PGE_1 did not increase DASMC proliferation, as determined on MTT assay, in the presence of 0 or 10% FBS (Figure 5B). Moreover, we found that milrinone did not enhance HA-mediated migration in DASMCs (Figure 6A). Milrinone also did not affect proliferation in HA-treated DASMCs (Figure 6B). Similarly, in ASMCs and PASMCs, neither milrinone nor PGE_1 increased HA production or cell migration and proliferation (Figures 4B,5). These findings suggest that PDE3 inhibitors do not promote HA production or cell migration or proliferation, although they do produce cAMP and dilate the DA.

PDE3a and PDE3b Highly Expressed in the Smooth Muscle Layer in Human DA Tissue

The expression pattern of PDE3s in human DA remains unknown. We examined PDE3a and PDE3b protein expression in the DA of 8 patients with CHD, such as interruption of the aortic arch, complex aortic coarctation, hypoplastic left ventricle, and asplenia. The DA of all patients had a strong immunoreaction for both PDE3a and PDE3b (Figure 7A). It has been demonstrated that PDE3a and PDE3b are abundantly expressed in the rat and human aorta.[25,26] The expression of PDE3a and PDE3b in the DAs was equivalent to that in the adjacent aortas (Figure 7B). This demonstrates that PDE3s are abundantly expressed in human patients with CHD of the type that may require long-term vasodilatotherapy prior to surgery.

Discussion

The present study has demonstrated that the PDE3 inhibitors milrinone and olprinone dilate the DA without causing apnea and have a longer duration of action than PGE_1. These findings are expected to apply to human patients, given that PDE3s are abundantly expressed in the DA tissue of infants

with CHD. Importantly, this study has shown for the first time that these PDE3 inhibitors do not promote HA production, cell migration, and cell proliferation in the DASMC, processes that potently induce IT and thus DA closure.[1] The PDE3 inhibitors are very unlikely to produce these unfavorable effects when used as DA dilators. Furthermore, these PDE3 inhibitors are already used in humans for other purposes.[9,10,13,14] Accordingly, they may serve as useful alternatives to PGE_1, the current means of keeping the DA patent.

PGE_1 increases the production of cAMP by activating G protein and adenylyl cyclase.[1,2,27] In contrast, milrinone increases the concentration of cAMP by inhibiting its breakdown.[7] Although both drugs increase cAMP and dilate the DA, PGE_1 induces HA production and subsequent migration in DASMCs while milrinone does not. We do not know the molecular mechanism underlying this difference between PGE_1 and the PDE inhibitors. It can be tentatively speculated, however, that they differ in terms of intracellular localization and thus in terms of coupling with other molecules, as recent studies have suggested.[28] Regardless of the mechanisms involved, it is known that PGE_1 and PGE_2 both increase cAMP production and induce HA production via increased expression of HA synthase 2,[1,5] and we found that a PDE4 inhibitor, rolipram, did not induce HA production (Figure 4B). Alternatively, increases in cGMP, which is also induced by milrinone, may play a role. These issues need to be further investigated in future studies.

Previous studies effectively demonstrated the vasodilatory effects of the PDE3 inhibitors milrinone, amrinone and cilostazol on the rat or sheep DA that underwent contraction by indomethacin.[15,16] In contrast, we have evaluated the effects of PDE3 inhibitors in the absence of indomethacin to examine the effects of PDE3 inhibitors in more relevant clinical settings. We also found, for the first time, that olprinone, a relatively new PDE3 inhibitor, dilates the DA. The present finding that these PDE3 inhibitors do not increase HA production is also novel, because this question had not been investigated previously.

The present study shows that milrinone does not induce SMC migration and proliferation in the DA (Figures 5,6). The present findings are, at least in part, consistent with those obtained using vascular SMCs from non-DA vessels. PDE3 inhibitors have elsewhere been shown to reduce proliferation and migration of vascular SMCs and to decrease the accumulation of synthetic/activated vascular SMCs in the intimal layers of damaged blood vessels.[7,29,30] Similarly, in peripheral PAs, PDE3 and PDE4 inhibition do not promote PASMC migration.[31] Furthermore, PDE3a deficiency caused G0/G1 cell cycle arrest in PDE3a knockout mice.[8]

PGE_1 is currently the sole DA dilator, but PGE_1-induced apnea or respiratory distress was noted in 18% of patients with CHD.[32] Respiratory depression was particularly common in infants weighing <2.0kg at birth who received PGE_1 therapy (42%).[22] The present study showed that milrinone and olprinone did not induce respiratory distress in rat neonates (Figure 3). Furthermore, no occurrence of apnea or respiratory distress due to PDE3 inhibitors has been previously reported.[9,10,13,14] Therefore, the PDE3 inhibitors are very unlikely to produce an unfavorable effect on respiration when used as DA dilators. It should be noted that PDE3 inhibitors have adverse effects, such as arrhythmia or hypotension.[33] Milrinone reduces the risk of low cardiac output syndrome for some pediatric patients after congenital heart surgery, but milrinone use is an independent risk factor for clinically significant tachyarrhythmias.[34] Although it was not feasible to examine arrhythmias and change in blood pressure in rat neonates in this study, careful further study is warranted to examine adverse effects.

It should be emphasized that both the PDE3a protein and the PDE3b protein were abundantly detected in the smooth muscle layer and the IT layer in all human DA samples tested, regardless of diagnosis or patient age at the time of operation (Figure 7). A previous study demonstrated that PDE3 inhibitors prevented DA closure in premature infants with persistent pulmonary hypertension.[15,35,36] Together with these findings, those of the present study suggest that PDE3 inhibitors can dilate the DA without inducing IT, and that they may serve as alternatives to PGE_1, the current DA vasodilator used for patients with DA-dependent CHD.

Acknowledgment

We are grateful to Yuka Sawada for excellent technical assistance.

Disclosure

This work was supported by grants from the Ministry of Health, Labor, and Welfare of Japan, a Grant-in-Aid for Scientific Research on Innovative Areas (22136009 to Y. Ishikawa and 23116541 to U. Yokoyama), the Ministry of Education, Culture, Sports, Science, and Technology of Japan (Y. Ichikawa, U. Yokoyama, M. Masuda and Y. Ishikawa), the Kitsuen Kagaku Research Foundation (Y. Ishikawa), the Yokohama Foundation for Advanced Medical Science (Y. Ichikawa and U. Yokoyama), the Takeda Science Foundation (U. Yokoyama and Y. Ishikawa), the Miyata Cardiac Research Promotion Foundation (U. Yokoyama), and the Mochida Memorial Foundation for Medical and Pharmaceutical Research (U. Yokoyama).

References

1. Yokoyama U, Minamisawa S, Quan H, Ghatak S, Akaike T, Segi-Nishida E, et al. Chronic activation of the prostaglandin receptor EP4 promotes hyaluronan-mediated neointimal formation in the ductus arteriosus. *J Clin Invest* 2006; **116:** 3026–3034.
2. Yokoyama U, Minamisawa S, Katayama A, Tang T, Suzuki S, Iwatsubo K, et al. Differential regulation of vascular tone and remodeling via stimulation of type 2 and type 6 adenylyl cyclases in the ductus arteriosus. *Circ Res* 2010; **106:** 1882–1892.
3. Smith GC. The pharmacology of the ductus arteriosus. *Pharmacol Rev* 1998; **50:** 35–58.
4. Yokoyama U, Minamisawa S, Ishikawa Y. Regulation of vascular tone and remodeling of the ductus arteriosus. *J Smooth Muscle Res* 2010; **46:** 77–87.
5. Sussmann M, Sarbia M, Meyer-Kirchrath J, Nusing RM, Schror K, Fischer JW. Induction of hyaluronic acid synthase 2 (HAS2) in human vascular smooth muscle cells by vasodilatory prostaglandins. *Circ Res* 2004; **94:** 592–600.
6. Mitani Y, Takabayashi S, Sawada H, Ohashi H, Hayakawa H, Ikeyama Y, et al. Fate of the "opened" arterial duct: Lessons learned from bilateral pulmonary artery banding for hypoplastic left heart syndrome under the continuous infusion of prostaglandin E1. *J Thorac Cardiovasc Surg* 2007; **133:** 1653–1654.
7. Maurice DH, Palmer D, Tilley DG, Dunkerley HA, Netherton SJ, Raymond DR, et al. Cyclic nucleotide phosphodiesterase activity, expression, and targeting in cells of the cardiovascular system. *Mol Pharmacol* 2003; **64:** 533–546.
8. Begum N, Hockman S, Manganiello VC. Phosphodiesterase 3A (PDE3A) deletion suppresses proliferation of cultured murine vascular smooth muscle cells (VSMCs) via inhibition of mitogen-activated protein kinase (MAPK) signaling and alterations in critical cell cycle regulatory proteins. *J Biol Chem* 2011; **286:** 26238–26249.
9. Klein L, O'Connor CM, Leimberger JD, Gattis-Stough W, Pina IL, Felker GM, et al. Lower serum sodium is associated with increased short-term mortality in hospitalized patients with worsening heart failure: Results from the Outcomes of a Prospective Trial of Intravenous Milrinone for Exacerbations of Chronic Heart Failure (OPTIME-CHF) study. *Circulation* 2005; **111:** 2454–2460.
10. Niemann JT, Garner D, Khaleeli E, Lewis RJ. Milrinone facilitates resuscitation from cardiac arrest and attenuates postresuscitation myocardial dysfunction. *Circulation* 2003; **108:** 3031–3035.
11. Greenberg B. Acute decompensated heart failure: Treatments and challenges. *Circ J* 2012; **76:** 532–543.

12. Thomas SS, Nohria A. Hemodynamic classifications of acute heart failure and their clinical application: An update. *Circ J* 2012; **76:** 278–286.
13. Bassler D, Choong K, McNamara P, Kirpalani H. Neonatal persistent pulmonary hypertension treated with milrinone: Four case reports. *Biol Neonate* 2006; **89:** 1–5.
14. Bassler D, Kreutzer K, McNamara P, Kirpalani H. Milrinone for persistent pulmonary hypertension of the newborn. *Cochrane Database Syst Rev* 2010; **(11):** CD007802.
15. Toyoshima K, Momma K, Imamura S, Nakanishi T. In vivo dilatation of the fetal and postnatal ductus arteriosus by inhibition of phosphodiesterase 3 in rats. *Biol Neonate* 2006; **89:** 251–256.
16. Liu H, Manganiello V, Waleh N, Clyman RI. Expression, activity, and function of phosphodiesterases in the mature and immature ductus arteriosus. *Pediatr Res* 2008; **64:** 477–481.
17. Yokoyama U, Minamisawa S, Adachi-Akahane S, Akaike T, Naguro I, Funakoshi K, et al. Multiple transcripts of Ca2+ channel alpha1-subunits and a novel spliced variant of the alpha1C-subunit in rat ductus arteriosus. *Am J Physiol Heart Circ Physiol* 2006; **290:** H1660–H1670.
18. Akaike T, Jin MH, Yokoyama U, Izumi-Nakaseko H, Jiao Q, Iwasaki S, et al. T-type Ca2+ channels promote oxygenation-induced closure of the rat ductus arteriosus not only by vasoconstriction but also by neointima formation. *J Biol Chem* 2009; **284:** 24025–24034.
19. Yokoyama U, Patel HH, Lai NC, Aroonsakool N, Roth DM, Insel PA. The cyclic AMP effector Epac integrates pro- and anti-fibrotic signals. *Proc Natl Acad Sci USA* 2008; **105:** 6386–6391.
20. Hoffman TM, Wernovsky G, Atz AM, Kulik TJ, Nelson DP, Chang AC, et al. Efficacy and safety of milrinone in preventing low cardiac output syndrome in infants and children after corrective surgery for congenital heart disease. *Circulation* 2003; **107:** 996–1002.
21. Taoka M, Shiono M, Hata M, Sezai A, Iida M, Yoshitake I, et al. Child with fulminant myocarditis survived by ECMO Support: Report of a child case. *Ann Thorac Cardiovasc Surg* 2007; **13:** 60–64.
22. Lewis AB, Freed MD, Heymann MA, Roehl SL, Kensey RC. Side effects of therapy with prostaglandin E1 in infants with critical congenital heart disease. *Circulation* 1981; **64:** 893–898.
23. Tananari Y, Maeno Y, Takagishi T, Sasaguri Y, Morimatsu M, Kato H. Role of apoptosis in the closure of neonatal ductus arteriosus. *Jpn Circ J* 2000; **64:** 684–688.
24. Boudreau N, Rabinovitch M. Developmentally regulated changes in extracellular matrix in endothelial and smooth muscle cells in the ductus arteriosus may be related to intimal proliferation. *Lab Invest* 1991; **64:** 187–199.
25. Reinhardt RR, Chin E, Zhou J, Taira M, Murata T, Manganiello VC, et al. Distinctive anatomical patterns of gene expression for cGMP-inhibited cyclic nucleotide phosphodiesterases. *J Clin Invest* 1995; **95:** 1528–1538.
26. Palmer D, Maurice DH. Dual expression and differential regulation of phosphodiesterase 3A and phosphodiesterase 3B in human vascular smooth muscle: Implications for phosphodiesterase 3 inhibition in human cardiovascular tissues. *Mol Pharmacol* 2000; **58:** 247–252.
27. Breyer RM, Bagdassarian CK, Myers SA, Breyer MD. Prostanoid receptors: Subtypes and signaling. *Annu Rev Pharmacol Toxicol* 2001; **41:** 661–690.
28. Houslay MD. Underpinning compartmentalised cAMP signalling through targeted cAMP breakdown. *Trends Biochem Sci* 2010; **35:** 91–100.
29. Netherton SJ, Jimmo SL, Palmer D, Tilley DG, Dunkerley HA, Raymond DR, et al. Altered phosphodiesterase 3-mediated cAMP hydrolysis contributes to a hypermotile phenotype in obese JCR: LA-cp rat aortic vascular smooth muscle cells: Implications for diabetes-associated cardiovascular disease. *Diabetes* 2002; **51:** 1194–1200.
30. Souness JE, Hassall GA, Parrott DP. Inhibition of pig aortic smooth muscle cell DNA synthesis by selective type III and type IV cyclic AMP phosphodiesterase inhibitors. *Biochem Pharmacol* 1992; **44:** 857–866.
31. Pullamsetti S, Krick S, Yilmaz H, Ghofrani HA, Schudt C, Weissmann N, et al. Inhaled tolafentrine reverses pulmonary vascular remodeling via inhibition of smooth muscle cell migration. *Respir Res* 2005; **6:** 128.
32. Meckler GD, Lowe C. To intubate or not to intubate? Transporting infants on prostaglandin E1. *Pediatrics* 2009; **123:** e25–e30.
33. Shin DD, Brandimarte F, De Luca L, Sabbah HN, Fonarow GC, Filippatos G, et al. Review of current and investigational pharmacologic agents for acute heart failure syndromes. *Am J Cardiol* 2007; **99:** 4A–23A.
34. Smith AH, Owen J, Borgman KY, Fish FA, Kannankeril PJ. Relation of milrinone after surgery for congenital heart disease to significant postoperative tachyarrhythmias. *Am J Cardiol* 2011; **108:** 1620–1624.
35. Yasuda K, Koyama N, Nomura T, Suzuki Y. Effects of phosphodiesterase 3 inhibitors to premature PDA. *J Jpn Soc Prem Newborn Med* 2004; **16:** 395 (in Japanese).
36. Nakamura M, Yamanouchi T, Taguchi T, Suita S. Effect of phosphodiesterase III inhibitor on persistent pulmonary hypertension of neonate associated with congenital diaphragmatic hernia: A case report. *J Jpn Soc Pediatr Surg* 2001; **37:** 1073–1077 (in Japanese).

Supplementary Files

Supplementary File 1

Figure S1. Quantitative RT-PCR of PDE3a, PDE3b, EP4 and IP in the DASMCs, ASMCs, PASMCs.

Please find supplementary file(s);
http://dx.doi.org/10.1253/circj.CJ-12-0215

J Pharmacol Sci **119**, 381 – 389 (2012)

Journal of Pharmacological Sciences

Full Paper

Pharmacological Stimulation of Type 5 Adenylyl Cyclase Stabilizes Heart Rate Under Both Microgravity and Hypergravity Induced by Parabolic Flight

Yunzhe Bai[1], Takashi Tsunematsu[1], Qibin Jiao[1], Yoshiki Ohnuki[2], Yasumasa Mototani[2], Kouichi Shiozawa[2], Meihua Jin[1], Wenqian Cai[1], Hui-Ling Jin[1], Takayuki Fujita[1], Yasuhiro Ichikawa[1], Kenji Suita[1], Reiko Kurotani[1,3], Utako Yokoyama[1], Motohiko Sato[1], Kousaku Iwatsubo[4], Yoshihiro Ishikawa[1,4], and Satoshi Okumura[1,2,*]

[1]*Cardiovascular Research Institute, Yokohama City University Graduate School of Medicine, Yokohama 236-0004, Japan*
[2]*Department of Physiology, Tsurumi University School of Dental Medicine, Yokohama 230-8501, Japan*
[3]*Biochemical Engineering, Faculty of Engineering, Yamagata University, Yonezawa, Yamagata 992-8501, Japan*
[4]*Cardiovascular Research Institute, Department of Cell Biology & Molecular Medicine and Medicine (Cardiology), New Jersey Medical School of UMDNJ, Newark, New Jersey 07103, USA*

Received April 25, 2012; Accepted June 21, 2012

Abstract. We previously demonstrated that type 5 adenylyl cyclase (AC5) functions in autonomic regulation in the heart. Based on that work, we hypothesized that pharmacological modulation of AC5 activity could regulate the autonomic control of the heart rate under micro- and hypergravity. To test this hypothesis, we selected the approach of activating AC5 activity in mice with a selective AC5 activator (NKH477) or inhibitor (vidarabine) and examining heart rate variability during parabolic flight. The standard deviation of normal R-R intervals, a marker of total autonomic variability, was significantly greater under micro- and hypergravity in the vidarabine group, while there were no significant changes in the NKH477 group, suggesting that autonomic regulation was unstable in the vidarabine group. The ratio of low frequency and high frequency (HF) in heart rate variability analysis, a marker of sympathetic activity, became significantly decreased under micro- and hypergravity in the NKH477 group, while there was no such decrease in the vidarabine group. Normalized HF, a marker of parasympathetic activity, became significantly greater under micro- and hypergravity in the NKH477 group. In contrast, there was no such increase in the vidarabine group. This study is the first to indicate that pharmacological modulation of AC5 activity under micro- and hypergravity could be useful to regulate the autonomic control of the heart rate.

Keywords: adenylyl cyclase isoform, autonomic nerve activity, parabolic flight, heart rate variability, microgravity

Introduction

Cardiac function is regulated by the autonomic nervous system. Sympathetic regulation leads to coupling of the β-adrenergic receptor (β-AR) and Gs, the G-protein responsible for stimulating activity of adenylyl cyclase (AC), a membrane-bound enzyme that catalyzes the conversion of ATP to cyclic AMP (cAMP), thereby stimulating protein kinase A (PKA) and ultimately increasing cardiac contractility and heart rate (HR) (1 – 5). Parasympathetic regulation counteracts these effects through the activation of the muscarinic receptor and Gi, the G-protein that can inhibit cardiac contractility and heart rate (6). The autonomic nervous system constitutes the two arms of regulation in the heart. We developed a mouse model with disruption of a major AC isoform (type 5) in the heart and demonstrated that type 5 AC (AC5) regulates cardiac function through the parasympa-

*Corresponding author. okumura-s@tsurumi-u.ac.jp
Published online in J-STAGE on July 31, 2012 (in advance)
doi: 10.1254/jphs.12102FP

thetic arm of the autonomic nervous system, as well as through the sympathetic arm (7 – 9).

The autonomic nervous system is known to be altered under microgravity (10) and hypergravity (11, 12). We have previously examined the role of AC5 in the regulation of the autonomic nervous system in the heart under micro- and hypergravity induced by parabolic flights using transgenic mouse models with AC5 overexpressed in the heart (AC5TG) or with disrupted AC5 (AC5KO) and analyzed heart rate variability during parabolic flight. Changes in heart rate variability (HRV) in response to micro- and hypergravity were augmented in AC5KO, but attenuated in AC5TG, suggesting that AC5 plays an important role in stabilizing heart rate control via autonomic regulation under gravitational stress (13).

We hypothesized that pharmacological regulation of AC5 activity could modulate the autonomic control of the heart rate under gravitational stress during parabolic flight. To test this hypothesis, we decided to examine the effect on HRV of activating or inhibiting AC5 activity in wild-type mice with a selective AC5 activator: 6-[3-(dimethylamino)propionyl]forskolin (NKH477) (14) or an AC5 inhibitor: vidarabine (15) during parabolic flight. We found that HR was stabilized by increasing AC5 activity with NKH477, but destabilized by decreasing AC5 activity with vidarabine under micro- and hypergravity during parabolic flight, in accordance with our previous findings using AC5TG and AC5KO.

We also examined the the ratio between low frequency (LF) and high frequency (HF), a marker of sympathetic activity, and normalized HF (nHF), a marker of parasympathetic activity during the parabolic flight and found that AC5 activity plays an important role to show continuous responses in these autonomic parameters such as LF/HF or nHF, under micro- and hypergravity (16).

Many astronauts suffer to varying degrees from symptoms suggestive of autonomic dysfunction such as nausea, vomiting, and dizziness during the early days of space flight (17), as well as showing severe orthostatic intolerance for several days after spaceflight (18, 19). The underlying molecular mechanism and appropriate treatment for the autonomic dysfunction in space and on earth after space flight remain unknown. However, not only trained astronauts but also normal subjects will stay in space in the near future. Thus, it is important to clarify the mechanism and to establish suitable treatment of autonomic dysfunction during and after spaceflight. This study is the first to demonstrate that pharmacological activation/inhibition of AC5 activity can regulate the autonomic control of the heart rate under micro- and hypergravity, indicating the importance of regulating AC5 activity for the treatment of autonomic dysfunction in space and on earth after spaceflight.

Materials and Methods

Parabolic flight experiment

Parabolic flight experiments were performed in a jet airplane operated by the Diamond Air Service in Nagoya using the same protocol previously employed by us (13). Briefly, in one parabolic flight, which lasted for approximately 1 h, 8 – 12 parabolas were performed in total with a 4 – 6-min interval between consecutive parabolas. At the end of each parabolic flight, mice were euthanized by cervical dislocation and replaced with the next mice. Parabolic flight was divided into five phases (Fig. 1). The first phase (I) was in normogravity (1 G, G: gravity), the second phase (II) was in hypergravity (1.3 G), the third phase (III) was in microgravity (0.03 G), the fourth phase (IV) was in hypergravity (1.8 G), and the fifth phase (V) was in normogravity (1 G). Each parabola provided 15 – 20 s of microgravity (phase III) and hypergravity (phase IV) and we evaluated data from the first parabola, except in Figs. 3B, 4B, 5B, 6B, in which the G force in the hypergravity phase (phase II) before the microgravity phase was kept below 1.3 G to avoid excessive gravity stress on mice and the effect of previous parabolas. During the experiment, the temperature in the plane was kept at 22°C ± 2°C and air pressure was 0.9 ± 0.1 atm.

Animals

Male C57BL/6CrSlc mice aged 4 months were used for this experiment (Japan SLC, Inc., Hamamatsu). The

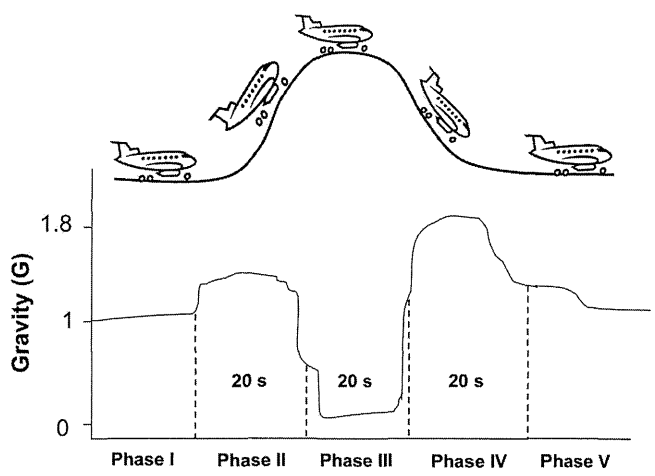

Fig. 1. Schematic representation of parabolic flight. Each parabola provided approximately 20 s of 0.03 G (G; gravity). Parabolic flight was divided into five phases. The first phase (I) was normogravity (1 G), the second phase (II) was hypergravity (1.3 G), the third phase (III) was microgravity (0.03 G), the fourth phase (IV) was hypergravity (1.8 G), and the fifth phase (V) was normogravity (1 G). The Y-axis indicates changes in gravity.

care and treatment of the animals were carried out according to the Japanese Government Animal Protection and Management Law (no. 105) and the Guidelines for Animal Experiments of Yokohama City University School of Medicine.

Experimental design and protocol

ECG recordings were obtained with a telemetric unit (PhysioTel; Data Sciences International, St. Paul, MN, USA). Infusion of NKH477 (1 $mg \cdot kg^{-1} \cdot day^{-1}$) (14), vidarabine (15 $mg \cdot kg^{-1} \cdot day^{-1}$) (15), or phosphate-buffered saline (PBS) as a control was done via an osmotic minipump (Model 2001; ALZET, Cupertino, CA, USA), which was implanted 16 h before the parabolic flight.

Time-domain measures

Conscious mice were separately placed in double-walled plastic cages, which were placed on a receiver in a special rack within the aircraft, and data from the freely moving mice were recorded by the data acquisition system during flight, as described previously by us (13). HRV measurements included mean HR, R-R interval (mean, max, minimum) and the standard deviation of normal R-R intervals (SDNN). The different G phases causes important changes in the R-R interval. Therefore, we also used the coefficient of variation (CV, %) as a normalized index of SDNN (CV-SDNN). SDNN (ms) = SD of all normal R-R intervals; CV-SDNN (%) = SDNN / mean R-R × 100.

Frequency-domain measures

In the frequency domain, the power spectral density was calculated by applying the fast Fourier transformation (FFT) to overlapping segments of the resampled data and by averaging the spectral results (16, 20). The FFT was calculated by using 512 points and half overlap with a Hann window. Cutoff frequencies divided the power spectrum into two main parts, LF (0.4 – 1.5 Hz) and HF (1.5 – 4.0 Hz) powers and were determined by multiplying the standard frequencies used in human studies by 10 to account for HR differences between mice and humans, as recommended by Gehrmann et al. (21). HF powers were normalized to account for differences in total power (TP) between animals by multiplying the power region of interest by 100 and dividing by the difference between TP and very LF power (0.0 – 0.4 Hz) (16).

Statistical analyses

All data are reported as the mean ± S.E.M. Statistical comparisons were performed with the Kruskal-Wallis nonparametric test followed by the Dunn test (Figs. 2, 3, 7, 8). Differences were considered significant at $P < 0.05$.

Results

Effect of parabolic flight on HR

Mean HR in the NKH477, vidarabine, and control groups were evaluated in each phase of parabolic flight during the first parabola. The HR in phase I in the NKH477 group was significantly higher than that in the control group [control group (n = 12): 558 ± 81 vs. NKH477 group (n = 8): 681 ± 38 bpm; $P < 0.01$] (Fig.

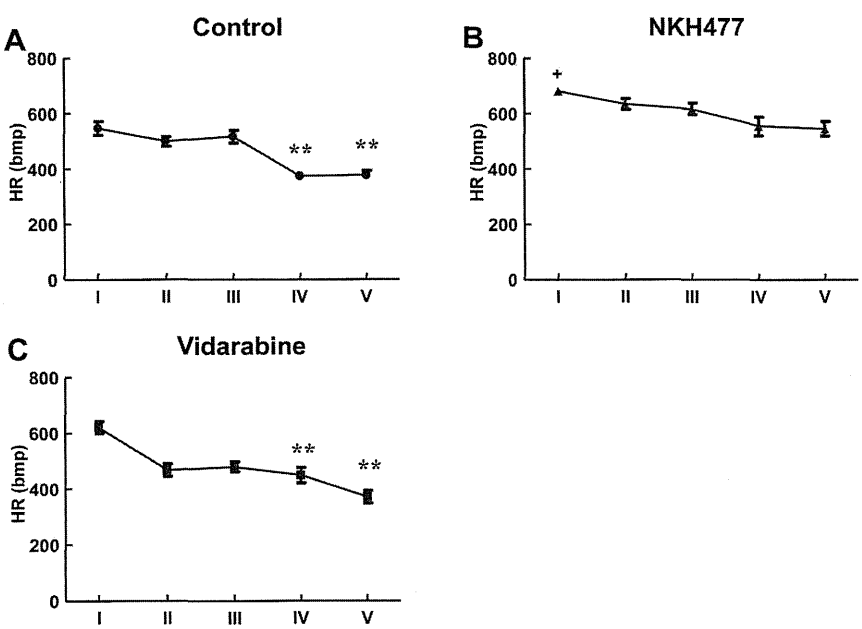

Fig. 2. Comparison of HR during parabolic flights. Comparison of HR among phases I, II, III, IV, and V in the control (n = 12) (A), NKH477 (n = 8) (B), vidarabine (n = 8) (C) groups during the first parabola. HR was compared between phase I and phase II, III, IV, or V in each group (**$P < 0.01$) and also between the control and NKH477 groups ($^{+}P < 0.05$).

2B), as previously found in AC5TG (13, 22). HR showed a significant decrease in later phases (IV – V) in the control and vidarabine groups, but there was no significant change in the NKH477 group, suggesting that HR was stabilized in the NKH477 group, compared with the other groups during parabolic flight.

Effect of parabolic flight on R-R interval of HRV

Maximum, mean, and minimum R-R intervals in the three groups were examined during the first and eighth parabolas (Fig. 3). Maximum, mean, and minimum R-R intervals, in general, increased gradually in later phases (I through IV) during the first parabola (Fig. 3A). When maximum, mean, and minimum R-R intervals were compared in each group during the first parabola, the degree of variability of the R-R interval was smaller in the NKH477 group (n = 8) and greater in the vidarabine group (n = 8) than that in the control group (n = 8). In the eighth parabola (Fig. 3B), the degree of variability remained unchanged in the vidarabine group (n = 8), suggesting that adaptations to micro- and hypergravity were impaired in the vidarabine group (10, 23).

For further analysis, the R-R intervals under normogravity (phase I), microgravity (phase III), and hypergravity (phase IV) were plotted by time (s) versus R-R (ms) interval in each group during the first (Figs. 4A, 5A, 6A) and eighth parabolas (Figs. 4B, 5B, 6B). The R-R intervals under normogravity (phase I) during the first parabola were stable in each group (Fig. 4A), but became more variable during the eighth parabola. However, the degree of variability was greater in the vidarabine group and smaller in the NKH477 group than that in the control group (Fig. 4B).

Under microgravity (phase III), the degree of variability was less in the NKH477 group, as compared with the other groups (Fig. 5A). However, the degree of variability was greater in the vidarabine group (n = 8) and smaller in the NKH477 group (n = 9) than that in the control group (n = 8) during the eighth parabola (Fig. 5B).

Under hypergravity (phase IV), the degree of variability showed a similar tendency to that under microgravity in the three groups during the first (Fig. 6A) and the eighth parabolas (Fig. 6B).

Taken together, these results may indicate that pharmacological activation of AC5 stabilizes the R-R intervals not only under microgravity but also under hypergravity during parabolic flight.

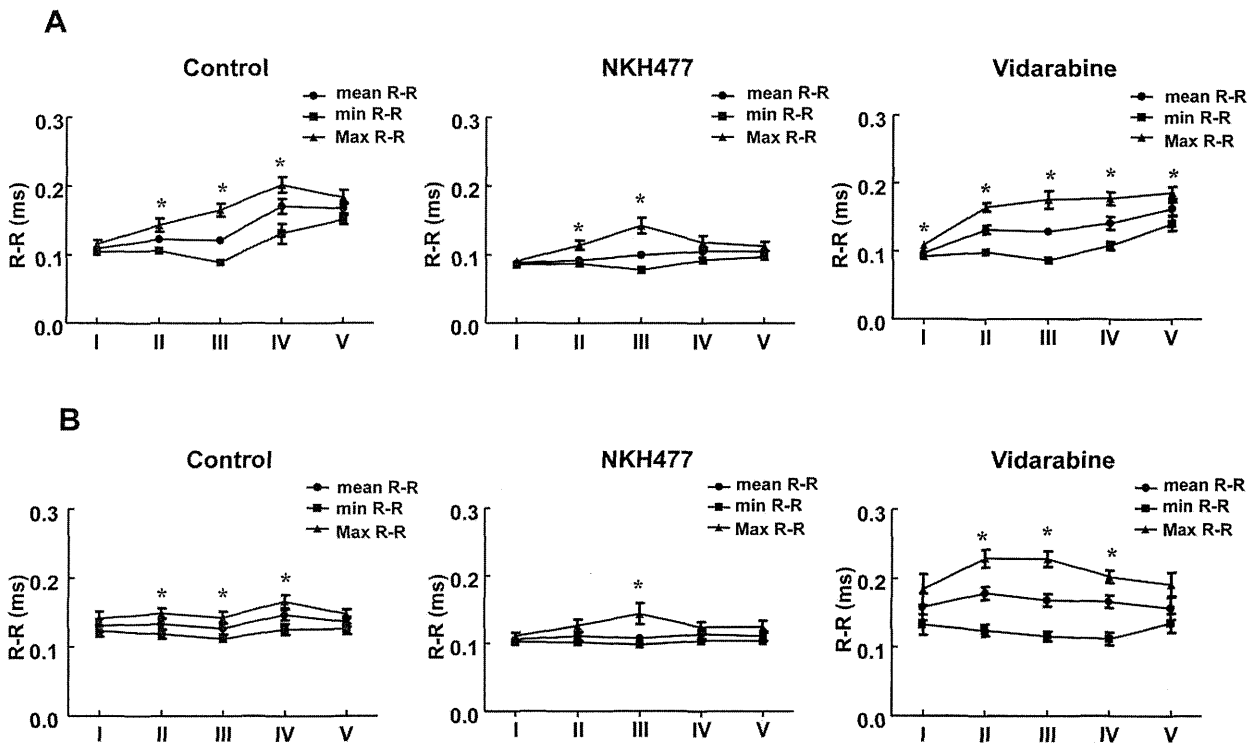

Fig. 3. Comparison of R-R interval during various phases of parabolic flights. Comparison of mean (mean), maximum (Max), and minimum (min) R-R intervals (ms) among phases I, II, III, IV, and V in the control (n = 8), NKH477 (n = 8 – 9), and vidarabine (n = 8) during the first parabola (A) and eighth parabola (B). Maximum R-R intervals were compared with the minimum R-R interval in each group (*$P < 0.05$).

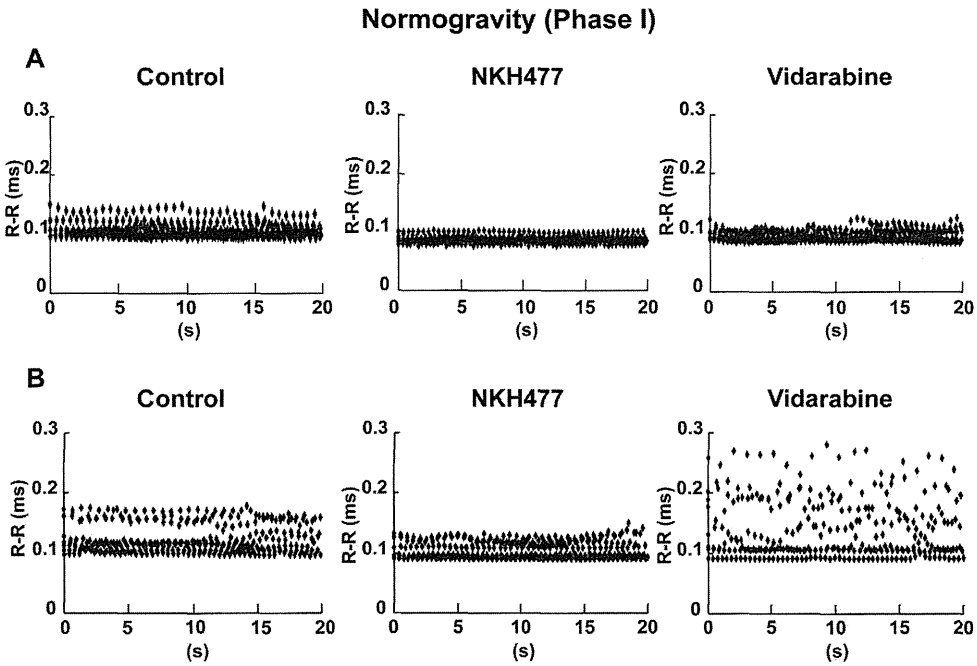

Fig. 4. Comparison of R-R interval under normogravity. R-R interval under normogravity (phase I) is shown by the plot of time (s) versus R-R interval (ms) in the control (n = 8), NKH477 (n = 8 – 9), vidarabine (n = 8) groups during the first (A) and eighth (B) parabolas.

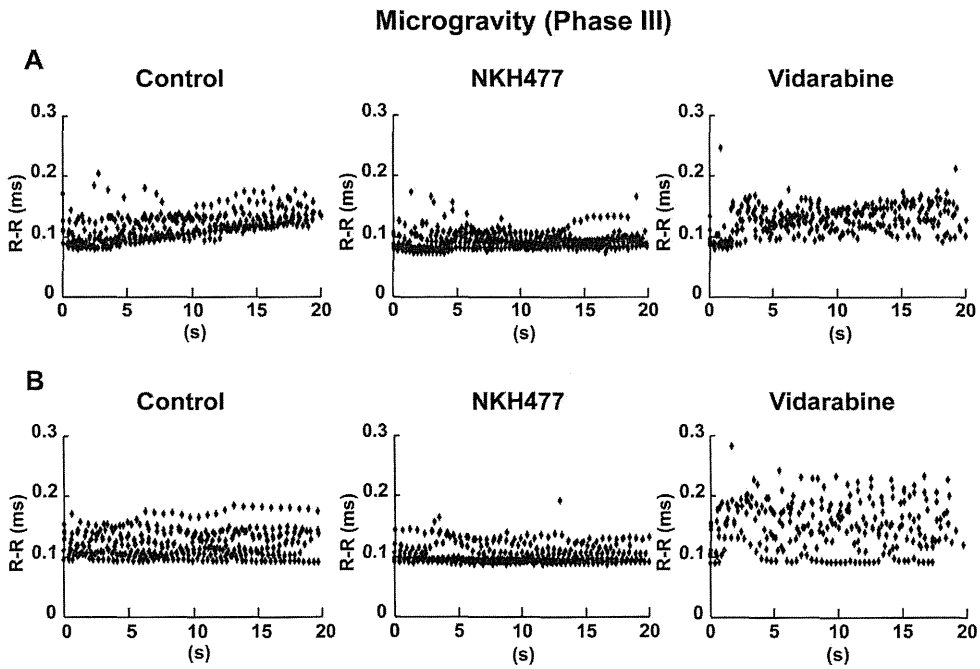

Fig. 5. Comparison of R-R interval under microgravity. Representative results under the microgravity (phase III) are shown by the plot of time (s) versus R-R interval (ms) in the control (n = 8), NKH477 (n = 8), and vidarabine (n = 8) groups during the first (A) and eighth (B) flights.

Effect of parabolic flight on SDNN of HRV

Because HR under gravitational stress is most likely regulated by the autonomic nervous system, we thus compared SDNN (Fig. 7A) and another parameter CV-SDNN (Fig. 7B) as a measure of total autonomic instability (24). SDNN and CV-SDNN were both significantly greater under microgravity (phase III) and hypergravity (phase II and IV) than those under normogravity (phase I) in each group. Notably, the absolute value of SDNN under microgravity (phase III) as well as hypergravity (phase IV) was strikingly greater in the vidarabine group (n = 8) and much smaller in the NKH477 group (n = 9) than that in the control group (n = 12). CV-SDNN showed similar behavior, indicating that increased AC5 activity stabilizes the autonomic control of the heart rate under gravitational stress.

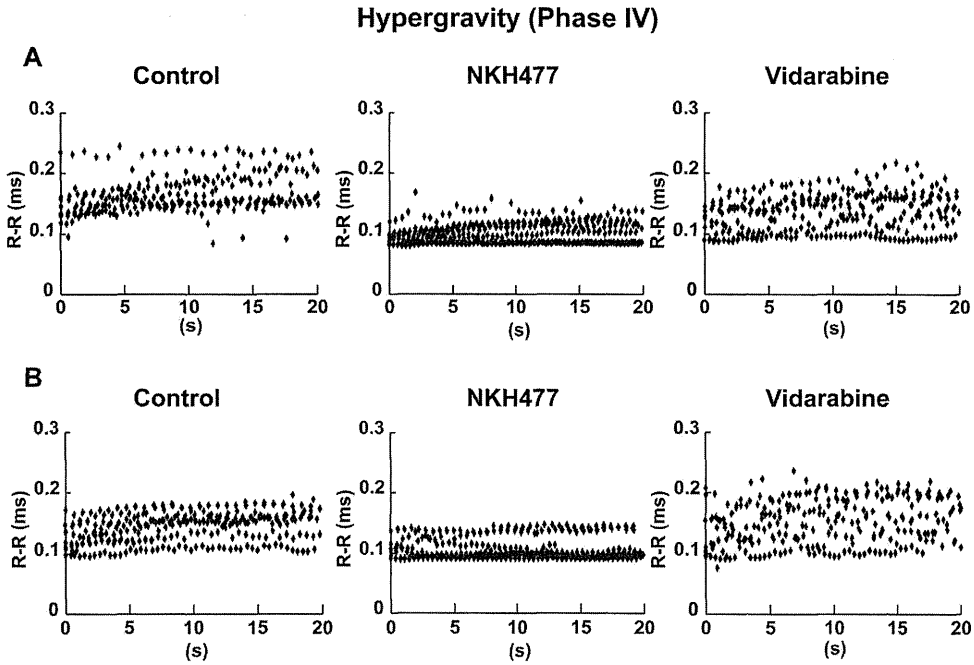

Fig. 6. Comparison of R-R interval under hypergravity. Representative results under the hypergravity (phase IV) are shown by the plot of time (s) versus R-R interval (ms) in the control (n = 8), NKH477 (n = 9), and vidarabine (n = 8) groups during the first (A) and eighth (B) flights.

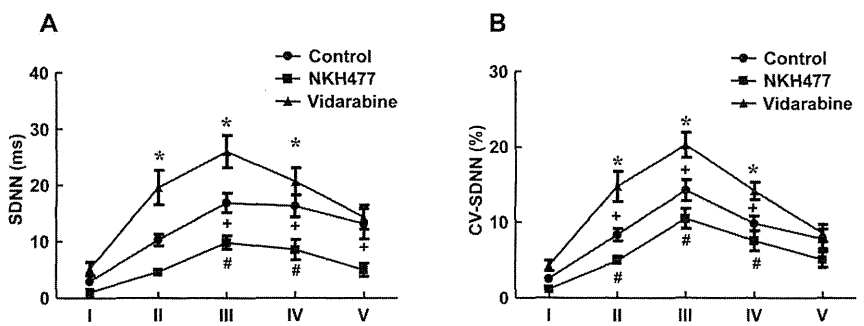

Fig. 7. Comparison of SDNN and CV-SDNN during parabolic flights. The standard deviation of normal R-R intervals (SDNN) (A) and coefficient of variation (CV, %) as a normalized index of SDNN (CV-SDNN) (B) during the first parabola. These indexes were compared between phase I and other phases in the control (n = 12), NKH477 (n = 9), and vidarabine (n = 8) groups ($^{+}$, *, $^{\#}P < 0.05$ vs. phase I).

Effect of parabolic flight on LF/HF of HRV

To further evaluate changes in autonomic nervous activity, we compared the ratio of LF to HF (LF/HF) in HRV analysis, an index of the sympathetic nervous tone in each phase of parabolic flight during the first parabola (16). When it was compared between normogravity (phase I) and microgravity (phase III), we found that LF/HF was significantly lower in phase I than that in phase III in the control and NKH477 groups (Fig. 8A) [control group (n = 10): phase I vs. phase III: 1.9 ± 0.4 vs. 0.9 ± 0.1 ms, $P < 0.05$; NKH477 group (n = 7): phase I vs. phase III, 2.1 ± 0.04 vs. 0.7 ± 0.05 ms, $P < 0.05$]. This was in agreement, at least in part, with previous studies in which decreased sympathetic nerve activity was demonstrated under microgravity in normal individuals (25). However, the vidarabine group did not show such a decrease [vidarabine group (n = 8): phase I vs. phase III: 1.9 ± 0.3 vs. 1.7 ± 0.3 ms, P = NS, not significant], suggesting that changes in sympathetic tone became small when AC5 activity was decreased with vidarabine.

Under hypergravity (phase IV), the ratio of LF/HF showed a similar tendency to that under microgravity in the three groups.

When it was compared between phase I (pre-parabolic flight) and phase V (post-parabolic flight), there was no difference in control group (phase I vs. phase V: 1.9 ± 0.4 vs. 1.7 ± 0.4 ms, P = NS) while it remained decreased in the NKH477 group (phase I vs. phase V: 2.1 ± 0.04 vs. 0.7 ± 0.1 ms, $P < 0.05$) (26). However, the vidarabine group showed no significant differences (phase I vs. phase V: 1.9 ± 0.3 vs. 1.9 ± 0.6 ms, P = NS).

Accordingly, sympathetic tone was transiently decreased under micro- and hypergravity in the control while it decreased in micro- and hypergravity and remained decreased in the NKH477 group even when gravity was normalized in the post-microgravity level flight (phase V); in contrast, such decreases were all ab-